AGU PUBLICATIONS

Geochemistry, Geophysics, Geosystems

RESEARCH ARTICLE
10.1002/2014GC005443

Key Points:
- "Unclean" foraminifera shells reliably record deep water Nd isotope compositions
- No evidence for seawater-sediment Nd isotope exchange off east New Zealand
- South Pacific lithogenic material mainly sourced from southeast Australia and south New Zealand

Correspondence to:
M. Molina-Kescher,
mmolina-kescher@geomar.de

Citation:
Molina-Kescher, M., M. Frank, and E. C. Hathorne (2014), Nd and Sr isotope compositions of different phases of surface sediments in the South Pacific: Extraction of seawater signatures, boundary exchange, and detrital/dust provenance, *Geochem. Geophys. Geosyst.*, *15*, 3502–3520, doi:10.1002/2014GC005443.

Received 2 JUN 2014
Accepted 1 AUG 2014
Accepted article online 5 AUG 2014
Published online 2 SEP 2014

Nd and Sr isotope compositions of different phases of surface sediments in the South Pacific: Extraction of seawater signatures, boundary exchange, and detrital/dust provenance

Mario Molina-Kescher[1], Martin Frank[1], and Ed C. Hathorne[1]

[1]GEOMAR Helmholtz Centre for Ocean Research Kiel, Kiel, Germany

Abstract The radiogenic isotope composition of neodymium (Nd) and strontium (Sr) are useful tools to investigate present and past oceanic circulation or input of terrigenous material. We present Nd and Sr isotope compositions extracted from different sedimentary phases, including early diagenetic Fe-Mn coatings, "unclean" foraminiferal shells, fossil fish teeth, and detritus of marine surface sediments (core-tops) covering the entire midlatitude South Pacific. Comparison of detrital Nd isotope compositions to deep water values from the same locations suggests that "boundary exchange" has little influence on the Nd isotope composition of western South Pacific seawater. Concentrations of Rare Earth Elements (REE) and Al/Ca ratios of "unclean" planktonic foraminifera suggest that this phase is a reliable recorder of seawater Nd isotope composition. The signatures obtained from fish teeth and "nondecarbonated" leachates of bulk sediment Fe-Mn oxyhydroxide coatings also agree with "unclean" foraminifera. Direct comparison of Nd isotope compositions extracted using these methods with seawater Nd isotope compositions is complicated by the low accumulation rates yielding radiocarbon ages of up to 24 kyr, thus mixing the signal of different ocean circulation modes. This suggests that different past seawater Nd isotope compositions have been integrated in authigenic sediments from regions with low sedimentation rates. Combined detrital Nd and Sr isotope signatures indicate a dominant role of the Westerly winds transporting lithogenic material from South New Zealand and Southeastern Australia to the open South Pacific. The proportion of this material decreases toward the east, where supply from the Andes increases and contributions from Antarctica cannot be ruled out.

1. Introduction

The radiogenic isotope compositions of Nd and Sr in seawater and sediments have been demonstrated to be useful tools to understand Earth surface processes given that they are not affected by biological fractionation or thermodynamic processes that potentially bias nutrient-based tracers [e.g., *Frank*, 2002]. Thus, they serve as tracers of present [e.g., *von Blanckenburg*, 1999; *Goldstein and Hemming*, 2003; *Rickli et al.*, 2009; *Stichel et al.*, 2012a; *Molina-Kescher et al.*, 2014] and past oceanic circulation regimes [e.g., *Rutberg et al.*, 2000; *Scher and Martin*, 2004; *Piotrowski et al.*, 2005, 2008, 2012; *Gutjahr et al.*, 2008; *Pahnke et al.*, 2008; *Basak et al.*, 2010; *Martin et al.*, 2012; *Pena et al.*, 2013]. Detrital silicate signatures trace continental weathering regimes, inputs, and transport [e.g., *Walter et al.*, 2000; *Franzese et al.*, 2006; *Roy et al.*, 2007; *Hemming et al.*, 2007; *Ehlert et al.*, 2011; *Fagel and Mattielli*, 2011; *Stumpf et al.*, 2011; *Asahara et al.*, 2012; *Dou et al.*, 2012; *Soulet et al.*, 2013], or dust input to the oceans [e.g., *Goldstein et al.*, 1984; *Greaves et al.*, 1994; *Grousset and Biscaye*, 2005, and references therein; *Delmonte et al.*, 2004; *Revel-Rolland et al.*, 2006; *Noble et al.*, 2012]. Radiogenic isotope signatures are obtained either directly from seawater, from authigenic seawater-derived phases such as carbonates, fish teeth, early diagentic Fe-Mn coatings of sediment particles, or from weathered terrigenous detrital silicate material.

The radiogenic isotope composition of Nd ($^{143}Nd/^{144}Nd$) is expressed in the epsilon (ε_{Nd}) notation: $\varepsilon_{Nd} = [(^{143}Nd/^{144}Nd_{sample}/^{143}Nd/^{144}Nd_{CHUR}) - 1]*10{,}000$, where CHUR stands for Chondritic Uniform Reservoir ($^{143}Nd/^{144}Nd = 0.512638$) [*Jacobsen and Wasserburg*, 1980]. The ε_{Nd} and Sr isotope composition of continental rocks varies as a function of age and rock type, therefore, allowing the distinction of regional and local sources of detrital silicate supplied from the continents and deposited on the ocean floor. Neodymium isotopes also serve as tracers of water masses as the characteristic Nd isotope composition of the different

continental source rocks is supplied to the surrounding oceans via rivers and dissolution of particles, thus transferring characteristic signatures to the ocean, which, together with the short oceanic residence time of Nd of 400–2000 years [*Tachikawa et al*., 2003; *Arsouze et al*., 2009; *Rempfer et al*., 2011], permits the flow paths and mixing of major water masses to be tracked. Nevertheless, the use of Nd isotopes is not without complications due to processes that affect their quasi-conservative behavior in seawater such as interactions with the sediments, particle dissolution, and reversible scavenging in the water column. Processes that cause the seawater isotope composition to change with no significant increase in the dissolved Nd concentration are referred to as "boundary exchange" [*Lacan and Jeandel*, 2005; *Singh et al*., 2012; *Stichel et al*., 2012b; *Pearce et al*., 2013]. These processes have been demonstrated to play an important role in the REE budget of the oceans [e.g., *Rempfer et al*., 2011], although their magnitude and the particular underlying mechanisms differ between oceanic regions and are an area of active research [e.g., *Wilson et al*., 2012, 2013; *Huang et al*., 2014; *Molina-Kescher et al*., 2014]. Efforts have been made to resolve these issues, such as expanding the knowledge of the natural cycle of trace elements in the ocean through new dedicated investigations and data along ocean sections, such as in the frame of the international GEOTRACES program [*SCOR Working Group*, 2007], or through modeling studies applying different parameterizations [*Siddall et al*., 2008; *Arsouze et al*., 2009; *Jones et al*., 2008; *Rempfer et al*., 2011, 2012].

For paleoceanographic studies, the reliable extraction of the seawater signal from sedimentary records [*Gutjahr et al*., 2007; *Elmore et al*., 2011; *Roberts et al*., 2010, 2012; *Piotrowski et al*., 2012; *Wilson et al*., 2013; *Kraft et al*., 2013] is crucial. Different approaches to obtain the seawater ε_{Nd} signal from authigenic, seawater-derived phases of marine sediments have been proposed, such as biogenic apatite of fish teeth [*Martin and Haley*, 2000; *Martin and Scher*, 2004], biogenic carbonates such as benthic foraminifera [*Klevenz et al*., 2008], deep sea corals [*van de Flierdt et al*., 2010], or authigenic Fe-Mn coatings of particles. The signatures contained in the latter are advantageous because they are widely available and allow high spatial and temporal coverage but have to be reliably separated from the "contaminant" detrital contributions. This has been achieved by only using authigenic Fe-Mn coatings of planktonic foraminifera [*Roberts et al*., 2010, 2012; *Tachikawa et al*., 2014] or by applying different leaching methods and reagents to bulk sediments [*Rutberg et al*., 2000; *Bayon et al*., 2002; *Gutjahr et al*., 2007; *Charbonnier et al*., 2012; *Wilson et al*., 2013]. Despite these effects, there have only been a few studies to date that directly compare bottom seawater Nd isotope compositions to those obtained from the sediments immediately below [*Tachikawa et al*., 2004; *Elmore et al*., 2011; *Roberts et al*., 2012; *Huang et al*., 2014].

Recently, new dissolved Nd isotope data sets have been published for the South Pacific [*Carter et al*., 2012; *Jeandel et al*., 2013; *Molina-Kescher et al*., 2014; *Rickli et al*., 2014], but sedimentary ε_{Nd} signatures have essentially not been studied in this very large region to date, the only exception being the eastern New Zealand margin [*Elderfield et al*., 2012; *Noble et al*., 2013]. In this study, we obtain the first ε_{Nd} signatures from different authigenic and detrital fractions of sediment core-tops in the open South Pacific and compare them directly to the signatures of overlying bottom seawater [*Molina-Kescher et al*., 2014]. Two important questions can be elucidated from this comparison of water and sedimentary ε_{Nd} data: (1) what role does seawater-sediment interaction play in the oceanic Nd cycle? This includes "boundary exchange," for which continental margins are considered to be both an important source and sink of Nd in the oceans [*Tachikawa et al*., 2003; *Lacan and Jeandel*, 2005; *Rempfer et al*., 2011] and (2) can the Nd isotope composition of bottom seawater in the South Pacific be reliably obtained from the sediments below in order to reconstruct past ocean circulation in this region? To resolve this second question, we compare results of four different extraction methods to obtain sedimentary seawater ε_{Nd} signatures ("unclean" planktonic foraminifera, fossil fish teeth/debris, "decarbonated," and "nondecarbonated" leachates of authigenic Fe-Mn coatings) and evaluate the importance of the two end-members that contribute to the authigenic sediment ε_{Nd} signatures: the detrital fraction of the sediment and the Nd dissolved in seawater. To corroborate the reliability of the extracting methods, we also examine Al/Ca ratios, REE patterns, and Sr isotope compositions to assess the absence of detrital contributions to the extracted solutions and to support the seawater origin of the Nd isotope ratios in the different phases.

The South Pacific is one of the regions where the lowest sedimentation rates globally occur. Below the carbonate compensation depth (CCD) located at around 4500 m water depth, the Southwest Pacific basin exhibits rates lower than 1 mm/kyr [e.g., *Schmitz et al*., 1986; *Glasby et al*., 1991, 2007; *Rea et al*., 2006]. This is a consequence of the isolation and the absence of large landmasses resulting in low atmospheric dust deposition compared to other oceanic regions [*Rea*, 1994; *Prospero*, 2002]. The small amount of dust that is supplied mainly consists of fine particles transported by the Southern Western Winds (SWW) from Australia

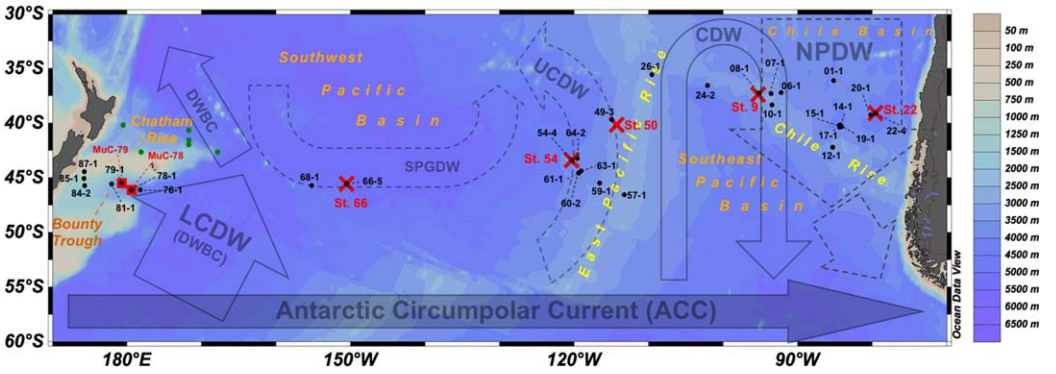

Figure 1. Study area with coarse bathymetry and the locations of the samples together with the schematic flow paths and flow directions of the main water masses below 1500 m (circulation patterns after *Kawabe and Fujio* [2010]). Black dots represent core-top sediment samples, red crosses and squares represent locations for which seawater ε_{Nd} analyses are available (data from *Molina-Kescher et al.* [2014]) whereby crosses are CTD-profiles and squares are bottom water samples obtained from multicorers. Green dots represent sediment samples presented in *Noble et al.* [2013]. Arrows represent water mass flow at middepths (dashed arrows), at the bottom (solid arrows), and occupying the entire water column (solid shaded arrow): AAC, Antarctic Circumpolar Current; LCDW, Lower Circumpolar Deep Water; DBWC, Deep Western Boundary Current; SPGDW, South Pacific Gyre-derived Deep Water; UCDW, Upper Circumpolar Deep Water; CDW, Circumpolar Deep Water; NPDW, North Pacific Deep Water.

and New Zealand [*Windom*, 1970; *Thiede*, 1979; *Fletcher and Moreno*, 2012; *Marx et al.*, 2014]. Transport of such particles by currents from other important continental regions that surround this enormous area, such as South America and Antarctica, may also contribute to the deep South Pacific. In order to track the provenance of the fine-grained terrigenous material (New Zealand, Australia, South America, and possibly also Antarctica) in different parts of this vast region, we combine Nd and Sr isotope compositions of the detrital silicate fraction of the sediment similar to studies carried out in the Atlantic section of the Southern Ocean [*Franzese et al.*, 2006].

2. Study Area, Samples, and Methods

The hydrography of the South Pacific is dominated by Southern Ocean-derived water masses at intermediate (AAIW) and bottom (LCDW) depths (ε_{Nd} ranging -8 to -9) whereas middepths between 1000 and 3500 m are occupied by more radiogenic Pacific-derived waters (Figure 1; see *Molina-Kescher et al.* [2014] for a detailed discussion). This is particularly the case in the eastern South Pacific where the main outflow of NPDW (average $\varepsilon_{Nd} = -5.9 \pm 0.3$) to the Southern Ocean occurs. In contrast, southeast of New Zealand, a Deep Western Boundary Current (DWBC) [e.g., *Carter et al.*, 1996] flowing to the north prevails that feeds the entire Pacific Ocean with circumpolar deep waters.

For this study, 31 core-top sediment samples were collected aboard the German RV SONNE during expedition SO213 that took place from December 2010 to March 2011 along a longitudinal transect between 36°S and 45°S extending over approximately 10,000 km from central Chile to New Zealand (Figure 1). All core-top sediment samples, from water depths between 542 and 5133 m (Table 1), represent undisturbed surface sediments as these were obtained using a multicore device, except sample 66-5 that corresponds to the first centimeters of the core-catcher of a piston core and thus its exact depth in the sediment is not known. Most samples were obtained above the carbonate compensation depth (CCD) and are therefore mainly composed of shells of foraminifera, as reflected by the typically high carbonate contents near 90% for the open ocean samples (Table 2). Biogenic opal is almost absent in all samples and the presence of detrital silicates is considerably higher in the samples obtained on the New Zealand Margin, ranging between 25% and 80%, and in two deep open ocean samples obtained below the CCD, 14-1 and 22-4, composed of 42% and 76% detrital silicates, respectively.

2.1. Methods Applied to the Extraction of Nd and Sr Isotope Signatures

Four different techniques were applied for the extraction of seawater-derived Nd and Sr isotope signatures from different phases of the sediment. In addition, detrital Nd and Sr isotope signatures were obtained from the same samples.

Table 1. Sample Information and Nd Isotope Composition for the Different Core-Top Fractions Analyzed in This Study With External Reproducibility (2σ)

				Detrital Fraction		Decarbonated Leachates		Nondecarbonated Leachates		Uncleaned Forams		Fish Teeth/Debris	
Sample	Latitude	Longitude	Depth (m)	ε_{Nd}	2σ	ε_{Nd}	2σ	ε_{Nd}	2σ	ε_{Nd}	2σ	ε_{Nd}	2σ
SO213-01-1	36°13′S	85°2′W	2806	−3.8	0.2	−4.7	0.4			−5.3	0.4		
SO213-06-1	37°21′S	92°23′W	2791	−4.5	0.2	−5.2	0.3			−5.3	0.4		
SO213-07-1	37°30′S	93°57′W	2571			−4.6	0.3						
SO213-08-1	37°29′S	95°21′W	2171	−4.8	0.2	−4.9	0.4	−4.5	0.3	−5.4	0.4	−4.9	0.7
SO213-10-1	38°36′S	93°43′W	2996	−5.0	0.2	−5.4	0.4			−5.6	0.4		
SO213-12-1	42°23′S	85°28′W	3016	−3.0	0.2	−4.0	0.4	−4.6	0.2	−4.6	0.4	−4.6	0.7
SO213-14-1	40°18′S	84°29′W	4052	−2.1	0.2	−4.6	0.4	−5.4	0.2	−5.6	0.3		
SO213-15-1	40°24′S	84°39′W	3246			−4.3	0.4						
SO213-17-1	40°37′S	84°30′W	2561	−2.7	0.2	−4.5	0.4			−4.5	0.4		
SO213-19-1	40°34′S	84°13′W	2951			−4.2	0.4						
SO213-20-1	39°27′S	80°18′W	2702	−2.9	0.2	−4.2	0.4			−4.5	0.4	−5.1	0.8
SO213-22-4	39°12′S	79°55′W	4125	−1.4	0.2	−2.0	0.2	−4.3	0.2				
SO213-24-2	36°57′S	102°07′W	3092	−5.7	0.2	−5.6	0.4	−5.8	0.3	−5.8	0.4		
SO213-26-1	35°60′S	109°55′W	2830	−5.6	0.2	−5.6	0.4	−5.7	0.2	−5.9	0.4		
SO213-49-3	39°57′S	114°1′W	3380	−5.5	0.2			−5.9	0.3	−5.8	0.4	−5.8	0.3
SO213-54-4	43°42′S	120°30′W	3840	−5.6	0.2	−5.6	0.2	−5.9	0.2	−6.0	0.3		
SO213-57-1	46°59′S	113°27′W	1194	−2.6	0.2	−6.6	0.4	−6.1	0.2	−6.3	0.3		
SO213-59-1	45°50′S	116°53′W	3159	−4.7	0.2	−5.8	0.4	−5.9	0.2	−5.8	0.4		
SO213-60-2	44°58′S	119°33′W	3468			−5.8	0.4			−6.3	0.3	−5.1	0.3
SO213-61-1	44°60′S	119°38′W	3616			−5.8	0.4						
SO213-63-1	44°40′S	119°05′W	3938	−5.6	0.2	−6.3	0.4	−5.9	0.2	−6.1	0.4		
SO213-64-2	43°24′S	119°53′W	3922			−6.2	0.4			−6.2	0.4		
SO213-66-5	45°23′S	151°42′W	5133	−5.2	0.2			−6.6	0.3				
SO213-68-1	45°7′S	155°17′W	1988	−5.2	0.2	−5.6	0.3			−5.5	0.4		
SO213-76-1	46°13′S	178°2′W	4337	−3.6	0.2	−3.7	0.3	−7.2	0.3				
SO213-78-1	46°15′S	179°37′W	3410	−3.4	0.2	−4.2	0.3	−7.0	0.3	−7.3	0.4		
SO213-79-1	45°51′S	179°34′E	3143	−4.0	0.2	−5.7	0.3	−8.1	0.3	−7.7	0.4		
SO213-81-1	45°60′S	178°0′E	2829	−4.2	0.2	−5.9	0.3	−7.8	0.3	−7.9	0.3		
SO213-84-2	45°7′S	174°35′E	992	−3.5	0.2	−2.9	0.3	−5.7	0.3	−5.4	0.3		
SO213-85-1	44°46′S	174°32′E	832	−3.5	0.2	−3.2	0.3	−5.9	0.3	−5.8	0.3		
SO213-87-1	44°5′S	174°6′E	542	−3.7	0.2	−3.0	0.3	−4.9	0.3				

2.1.1. Ferromanganese Coatings of Bulk Sediments

The first technique employed was the extraction of the seawater Nd and Sr isotopic signatures from authigenic ferromanganese coatings of the bulk sediment (~3 g) applying the leaching protocol of *Stumpf et al.* [2010]. The procedure consists of an initial double rinsing of the freeze-dried bulk sediment with deionized water followed by removal of the carbonate fraction of the sediment using acetic acid buffered with Na-acetate. The ferromanganese coatings were subsequently dissolved in a 0.05 *M* hydroxylamine hydrochloride/15% acetic acid solution (HH) buffered to pH 3.6 with NaOH. This method was applied for 29 samples for Nd and Sr isotope analysis and for three samples only for Nd analysis. We will refer to this method as "decarbonated leaching," which is distinct from the "nondecarbonated leaching" method, hereafter referred as "leaching," consisting of the same procedure described above but omitting the initial carbonate removal step. This second method was used for 19 samples only for analysis of Nd isotope compositions.

2.1.2. Planktonic Foraminifera With Ferromanganese Coatings

Between 25 and 75 mg of mixed species whole planktonic foraminifera shells were hand picked from the >250 μm size fraction under a light microscope from 22 different locations. Samples were subsequently cracked between glass plates, observing with a binocular to ensure that all chambers were opened and were ultrasonicated several times in deionized water and then in methanol to ensure the removal of most of the clays and silicate particles. The carbonates and associated ferromanganese coatings of the samples were then progressively dissolved by stepwise addition of dilute nitric acid (in total ~2 mL 0.5 *M* HNO_3). The solution was then centrifuged to ensure removal of the smallest detrital particles. A very similar procedure was named "unclean forams" by *Roberts et al.* [2010], who used picked planktonic forams, from which detrital silicate had been removed to analyze the Nd of the carbonate fraction together with Fe-Mn coatings [e.g., *Palmer and Elderfield*, 1985, 1986]. We will use the same term in our study to indicate that a reductive

Table 2. Sr Isotope Compositions, Aluminum to Calcium Ratios for Planktonic "Unclean" Foraminifera, % of Lithogenic Material and Available Radiocarbon Ages for the Core-Top Samples Analyzed in This Study[a]

Sample	Depth (m)	% of Carbon (Organic + $CaCo_3$)	% of SiO_2 (Opal)	% of Detrital Silicate	$^{87}Sr/^{86}Sr$ Detritus	2σ s.d.	$^{87}Sr/^{86}Sr$ Decarbonated Leachates	2σ s.d.	Al/Ca Unclean Foram (μmol/mol)	^{14}C Date (Y.b.p.)
01-1	2806	92	B.d.l.	8	0.70827	0.00002	0.70928	0.00003	B.d.l.	7982 ± 217
06-1	2791	94	2	4			0.70919	0.00003	B.d.l.	
07-1	2571	91	4	5			0.70966	0.00003		16261 ± 542
08-1	2171	94	B.d.l.	6	0.70895	0.00002	0.70918	0.00002	B.d.l.	17267 ± 606
10-1	2996	94	1	5			0.70918	0.00002	B.d.l.	
12-1	3016	90	3	7	0.70847	0.00002	0.70917	0.00003	1	
14-1	4052	58	B.d.l.	42					42	
15-1	3246	92	4	4			0.70917	0.00003		
17-1	2561	94	1	5	0.70867	0.00002	0.70920	0.00003	B.d.l.	24226 ± 811
19-1	2951	94	4	2			0.70920	0.00003		
20-1	2702	92	1	7	0.70796	0.00002	0.70914	0.00003	9	4142 ± 259
22-4	4125	23	1	76	0.70655	0.00002	0.70920	0.00003		
24-2	3092	94	B.d.l.	6			0.70920	0.00003	B.d.l.	
26-1	2830	82	1	17	0.70953	0.00002	0.70925	0.00003	B.d.l.	
49-3	3380								B.d.l.	
54-4	3840	92	B.d.l.	8	0.70982	0.00002	0.70938	0.00003	7	
57-1	1194	94	B.d.l.	6	0.70873	0.00002	0.70919	0.00003	B.d.l.	
59-1	3159	94	2	4					B.d.l.	8001 ± 210
60-2	3468	93	2	5	0.70934	0.00004	0.70919	0.00003		11169 ± 246
61-1	3616	90	3	7						
63-1	3938	87	6	7	0.7095	0.00002	0.70953	0.00003	B.d.l.	
64-2	3922	89	5	6			0.70920	0.00003	3	
66-5	5133									
68-1	1988	94	1	5	0.70936	0.00002	0.70921	0.00002	B.d.l.	
76-1	4337	18	12	70	0.70832	0.00002	0.70906	0.00002		
78-1	3410	46	2	52	0.70825	0.00002	0.70919	0.00002	47	
79-1	3143	67	3	30	0.70933	0.00002	0.70941	0.00002	41	
81-1	2829	73	3	24	0.70910	0.00002	0.70940	0.00002	B.d.l.	
84-2	992	41	2	57			0.70918	0.00002	362	4952 ± 238
85-1	832	35	1	64	0.70716	0.00002	0.70945	0.00002	229	
87-1	542	17	3	80	0.70766	0.00002	0.70906	0.00002		

[a]2σ s.d. = 2* sigma standard deviation, B.d.l. = below detection limit, Y.b.p. = years before present.

cleaning step for the dissolution of the coatings was not applied but that the ε_{Nd} signature of the combined foraminiferal carbonate and coatings was measured. As demonstrated in many settings [e.g., *Roberts et al*., 2010, 2012; *Kraft et al*., 2013; *Tachikawa et al*., 2014], this method provides reliable bottom water signatures given that the Nd concentrations in the calcite are negligible compared to those in the coatings, which precipitate and equilibrate in bottom waters.

2.1.3. Fish Teeth/Debris

Fish teeth and debris were found in the same size fraction as the foraminferal shells in five samples. These were hand picked and separated from detrital and carbonate particles by rinsing with deionized water and methanol to be finally digested in 6 *M* HCl [e.g., *Martin and Scher*, 2004].

2.1.4. Detrital Silicate Fraction

After application of the "decarbonated" leaching method described above, a second HH leach of 24 h was applied to those samples chosen for detrital silicate analyses in order to ensure that all Fe-Mn oxides were removed [e.g., *Innocent et al*., 1999; *Bayon et al*., 2002; *Gutjahr et al*., 2007]. This resulted in a fine-grained residue only consisting of the lithogenic detrital silicate fraction that was treated first with aqua regia and subsequently completely digested in a mixture of concentrated nitric and hydrofluoric acid similar to *Stumpf et al*. [2011]. In total, 26 samples were prepared for analysis of detrital Nd isotopes and 18 samples for detrital Sr isotopes.

2.2. Column Chemistry and Determination of Isotopic Signatures

Nd and Sr were separated from other elements applying a two-step ion chromatographic separation. The solutions resulting from the different extracting methods were brought through columns filled with 0.8 mL of Biorad® AG50W-X12 resin (200–400 μm mesh-size) [*Barrat et al*., 1996] to separate REEs and Sr. The

Table 3. REE Concentrations Normalized to PAAS [*Taylor and McLennan*, 1985] Measured on "Uncleaned" Planktonic Foraminifera Samples

Sample	Latitude	Longitude	Depth (m)	La	Ce	Pr	Nd	Sm	Eu	Gd	Tb	Dy	Ho	Er	Tm	Yb	Lu	Ce/Ce*
SO213-01-1	36°13′S	85°2′W	2806	2.14	0.35	2.00	2.41	3.08	3.89	4.39	4.93	5.34	5.55	6.27	6.60	6.28	6.10	0.17
SO213-06-1	37°21′S	92°23′W	2791	2.22	0.15	2.10	2.63	3.31	4.23	4.74	5.04	5.61	5.60	6.34	6.80	6.49	5.89	0.18
SO213-08-1	37°29′S	95°21′W	2171	2.30	0.22	2.07	2.60	3.15	4.08	4.74	5.14	5.91	6.36	6.79	7.66	7.33	6.68	0.13
SO213-10-1	38°36′S	93°43′W	2996	2.70	0.23	2.75	3.38	4.17	5.22	6.08	6.50	7.20	7.18	7.77	8.25	7.89	7.09	0.15
SO213-12-1	42°23′S	85°28′W	3016	2.66	0.49	2.69	3.68	4.34	4.96	5.85	6.47	6.81	7.11	7.75	7.93	7.93	4.49	0.13
SO213-14-1	40°18′S	84°29′W	4052	1.33	0.20	1.71	2.06	2.60	3.07	3.41	3.48	3.37	3.17	3.28	3.55	3.22	2.91	0.07
SO213-17-1	40°37′S	84°30′W	2561	2.17	0.31	2.06	2.59	3.15	4.21	4.70	4.96	5.61	5.93	6.47	6.81	6.98	6.26	0.10
SO213-20-1	39°27′S	80°18′W	2702	2.52	0.31	2.15	2.67	3.28	3.97	4.75	5.24	5.97	5.99	6.46	7.33	7.11	6.62	0.08
SO213-24-2	36°57′S	102°07′W	3092	2.38	0.12	2.51	2.95	3.82	4.75	5.40	5.99	6.60	6.43	7.09	7.60	7.38	6.63	0.05
SO213-26-1	35°60′S	109°55′W	2830	1.70	0.04	1.74	2.13	2.82	3.51	4.12	4.52	5.07	5.26	5.69	6.03	5.78	5.38	0.02
SO213-49-3	39°57′S	114°1′W	3380	2.64	0.12	2.89	3.48	4.46	5.46	5.86	6.63	6.89	6.79	7.19	7.42	7.08	6.65	0.04
SO213-54-4	43°42′S	120°30′W	3840	2.93	0.49	3.51	4.10	5.35	6.16	6.58	6.97	6.95	6.50	6.82	7.01	6.40	6.11	0.15
SO213-57-1	46°59′S	113°27′W	1194	0.93	0.17	0.83	0.99	1.23	1.59	1.86	1.93	2.26	2.39	2.63	2.68	2.62	2.44	0.19
SO213-59-1	45°50′S	116°53′W	3159	1.54	0.14	1.41	1.76	2.16	2.64	3.23	3.20	3.52	3.68	4.00	4.34	4.20	3.87	0.10
SO213-63-1	44°40′S	119°05′W	3938	2.09	0.27	2.43	2.90	3.70	4.40	4.71	4.93	5.01	4.77	4.83	4.70	4.62	4.02	0.12
SO213-64-2	43°24′S	119°53′W	3922	2.53	0.37	3.26	3.91	5.18	5.82	6.12	6.43	6.54	5.89	5.93	6.14	5.52	5.00	0.13
SO213-68-1	45°7′S	155°17′W	1988	2.11	0.31	1.74	2.15	2.65	3.27	3.97	4.42	4.99	5.33	5.83	6.25	6.20	5.77	0.16
SO213-78-1	46°15′S	179°37′W	3410	2.65	0.62	2.78	3.27	4.20	4.81	5.38	5.57	5.84	5.66	5.82	5.83	5.79	5.26	0.23
SO213-79-1	45°51′S	179°34′E	3143	1.79	0.37	1.75	2.06	2.65	3.01	3.56	3.68	3.90	3.90	4.06	4.26	4.01	3.81	0.21
SO213-81-1	45°60′S	178°0′E	2829	1.84	0.34	1.68	2.00	2.46	2.84	3.46	3.76	3.84	3.90	4.18	4.44	4.18	4.06	0.20
SO213-84-2	45°7′S	174°35′E	992	1.30	0.56	1.31	1.55	1.90	2.14	2.64	2.74	2.85	2.80	3.09	3.14	2.92	2.85	0.43
SO213-85-1	44°46′S	174°32′E	832	1.02	0.44	1.00	1.18	1.40	1.64	2.11	2.09	2.23	2.20	2.41	2.41	2.45	1.99	0.43
$Ce/Ce^* = 2*[Ce_{PAAS}]/([La_{PAAS}] + [Pr_{PAAS}])$			% 2* sigma →	8	8	8	8	9	9	6	8	6	7	7	33	8	2	

solutions containing Nd and Sr were further purified using Eichrom® Ln Spec resin (50–100 μm mesh-size, 2 mL resin bed) [*Le Fevre and Pin*, 2005] and Eichrom Sr Spec resin [*Horwitz et al*., 1992], respectively. Isotopic ratios of both elements were measured on a Nu plasma MC-ICPMS at GEOMAR, using ratios of 0.7219 for $^{146}Nd/^{144}Nd$ and of 0.1194 for $^{88}Sr/^{86}Sr$ to correct for instrumental mass bias. Nd and Sr isotope ratios were corrected for Sm and ^{86}Kr, ^{87}Rb interferences, respectively. The results were normalized to the accepted values of 0.512115 (JNdi-1 standard [*Tanaka et al*., 2000]) for $^{143}Nd/^{144}Nd$ and of 0.710245 (NIST NBS987) for $^{87}Sr/^{86}Sr$. The external reproducibilities (2σ) of the $^{143}Nd/^{144}Nd$ and $^{87}Sr/^{86}Sr$ measurements during each session ranged between 0.2 and 0.4 ε_{Nd} units and between 0.00002 and 0.00006, respectively, as assessed by repeated measurements of the above standards matching sample concentrations (see Tables 1 and 2).

2.3. Determination of Al/Ca Ratios and REE Concentrations on "Unclean" Foraminifera Cuts

Al/Ca and REE concentrations on "unclean" foraminifera were measured on an Agilent 7500ce ICP-MS in the same laboratory and using the same methods described in *Kraft et al*. [2013]. Briefly, ^{27}Al was measured simultaneously with other elements on samples diluted to 10 ppm Ca content following a first step to measure the Ca concentration of the samples. Element/Ca ratios were calculated from intensity ratios [*Rosenthal et al*., 1999] calibrated using standards with similar ratios to those found in foraminifera. The 2σ uncertainty was 6–7% for Al/Ca ratios. REE concentrations were obtained using an online preconcentration (OP) ICP-MS technique modified from *Hathorne et al*. [2012] using a "seaFAST" system (Elemental Scientific Inc.) coupled to the ICP-MS on samples diluted to a Ca concentration of 25 ppm. The 2σ uncertainty based on repeated measurement of a sample averaged 9% (see Table 3 for all elements).

2.4. ^{14}C Dating

Eight of the core-tops including at least one sample for each of the different areas and depths investigated in this study were radiocarbon dated (see areas in Figure 4). The analyses were carried out by the Leibniz Labor at Christian-Albrechts University Kiel on 1–1.4 mg of hand-picked mixed planktonic foraminiferal shells using accelerator mass spectrometry (AMS) and following the procedure after *Stuiver and Polach* [1977], which briefly consists in the release of ^{14}C, ^{13}C, and ^{12}C in form of CO_2 gas of the samples and comparison to known concentrations of the same isotopes of a standard (Oxalic Acid II), correcting for isotope fractionation by simultaneously measuring the $^{13}C/^{12}C$ ratio. ^{14}C ages were converted to calendar age using

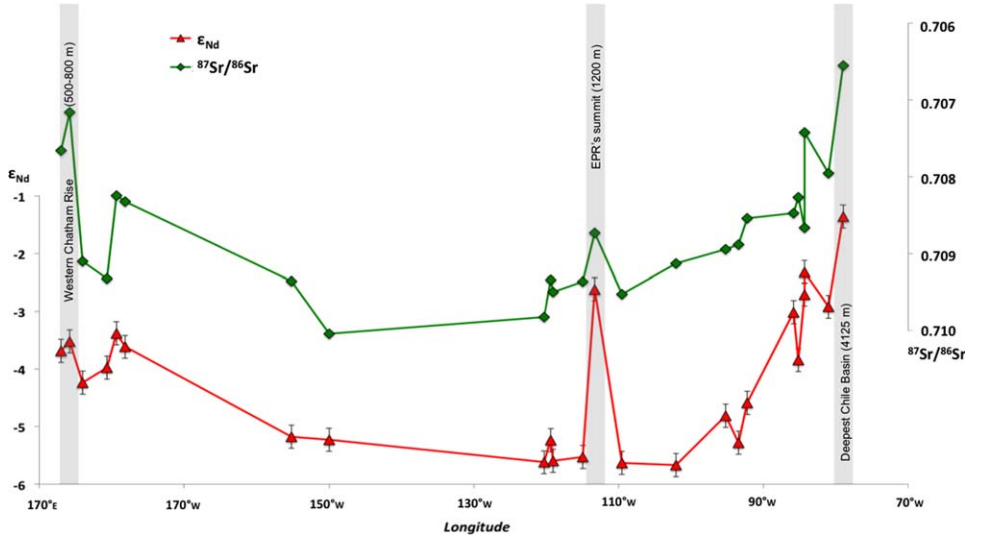

Figure 2. Spatial distribution of surface sediment detrital Nd and Sr isotope compositions in the South Pacific along the longitudinal section of SO213. The most radiogenic (unradiogenic) Nd (Sr) samples are highlighted by gray bars indicating their location and depth.

the radiocarbon calibration program CALIB 7.0 [*Stuiver and Reimer*, 1993; *Reimer et al*., 2013] with a ΔR correction of 560 years appropriate for this region [*Bard*, 1988].

3. Results

3.1. Neodymium and Strontium Isotope Composition of the Detrital Silicate Fraction

Detrital ε_{Nd} signatures (Table 1) show the most positive ε_{Nd} signatures at the locations nearest to the continental landmasses (Figure 2), ranging from -3 to -4 off New Zealand and from -1 to -4 in the Chile basin. The signatures become significantly less radiogenic as the distance from the continents increases, with the marked exception of station 57-1, located at the summit of the East Pacific Rise (EPR), which shows an ε_{Nd} value of -2.6 pointing to a significant contribution of mantle-derived rocks. Compared to the seawater signatures at the same or nearby stations [*Molina-Kescher et al*., 2014], the detrital ε_{Nd} signatures show more radiogenic values than the bottom waters for the entire study area (Figure 3). The difference between bottom waters and detrital Nd isotopic compositions varies between 6 and 1 ε_{Nd} units, with the largest differences found in the New Zealand margin (Figure 3a), the Chile Rise (Figure 3d), and deep Chile Basin (Figure 3e). The smallest difference occurs in deep East Pacific Rise area (Figure 3c) and between sample 68-1 and water sample 66–2200, both obtained in the center of the Southwest Pacific Basin near 2000 m water depth (Figure 3b).

The pattern observed for Nd isotopes is mirrored by the detrital Sr isotope compositions (Figure 2). The least radiogenic values occur near the continental margins: 0.70655 for the sample closest to Chile (22-2) and 0.70716 and 0.70766 for the two westernmost samples (87-1 and 85-1, respectively) located on the western Chatham Rise, whereas the values in the central South Pacific range from 0.709 to 0.710. The detrital Sr isotope signature of sample 57-1 is significantly less radiogenic than neighboring samples also pointing to a contribution of mantle rocks, however, with a less pronounced difference than in the case of Nd isotopes. This exceptional and marked difference toward less (more) radiogenic Sr (Nd) isotope compositions of sample 57-1 is due to an increased abundance of black basaltic particles of around 5% as observed under a light microscope. These particles are in the same size range as the foraminifera that compose around 95% of the sample and most likely originate from the Mid Oceanic Ridge (MORB). This finding points to submarine volcanic eruptions contributing to the sediment close to the active hydrothermal regions, in this case, the summit of the East Pacific Rise. This supports previous evidence of explosive eruptions at mid-ocean ridges [*Clague et al*., 2009; *Helo et al*., 2011]. Similar particles were not found in the other samples of this study.

3.2. Neodymium and Strontium Isotope Signatures in Leachates, Foraminifera, and Fish Teeth

Applying the four different extraction methods to obtain authigenic bottom water ε_{Nd} signatures from the sediments, all the data are systematically more radiogenic than those of the seawater Nd isotope

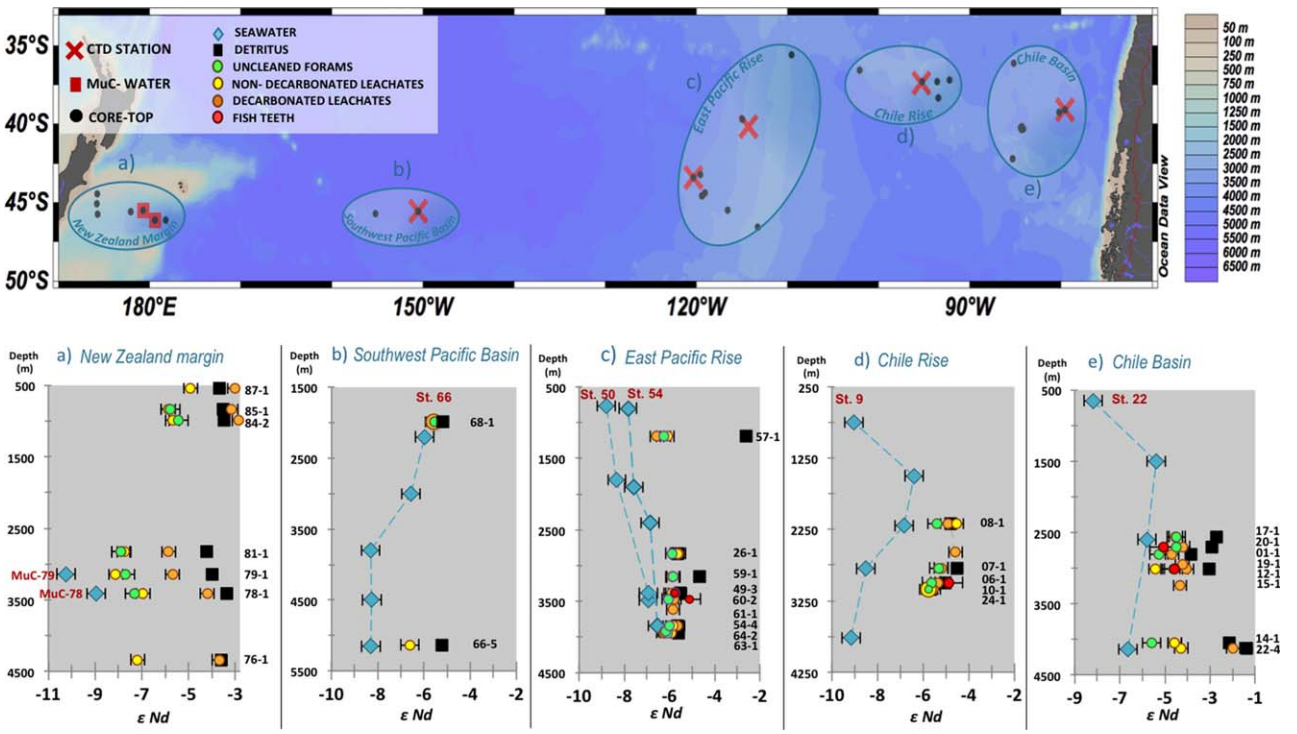

Figure 3. Nd isotope compositions with corresponding 2σ external reproducibilities for seawater (data from *Molina-Kescher et al*. [2014]), detrital fractions and the different methods applied for the extraction of authigenic, seawater-derived ε_{Nd} signatures plotted against water depth. The data are grouped in five different plots that correspond to specific regions marked by blue circles on the map on top. Every sample is identified to the right of the plots. Symbols are defined on the legend at the top left corner of the figure. The nomenclature of the samples on the map is provided in Figure 1.

compositions at the same locations and depths. The offsets, however, vary substantially between different methods and areas. The best agreement between the Nd isotope composition of seawater and authigenic sediments is observed on the East Pacific Rise (Figure 3c) and in the Chile Basin (Figure 3e), despite that in the later case the difference between both potential end-members (detrital silicate and seawater) is up to 5 ε_{Nd} units in the deeper areas. The largest difference between the extracted authigenic signal and the bottom waters of 2–3 ε_{Nd} units is observed above the Chile Rise (Figure 3d). In this case, the authigenic sediment signatures are identical within error to the detrital ε_{Nd} signatures. Generally, the results of the "decarbonated" leaching method were most different from the seawater signatures (2–5 ε_{Nd} units, especially in near coastal regions, such as at the New Zealand Margin (Figure 3a). These data in most cases closely match those of the detrital silicates whereas the "unclean" forams and "non-decarbonated" leachates only differ by 2 ε_{Nd} units from the water and by 3 ε_{Nd} units from the detritus.

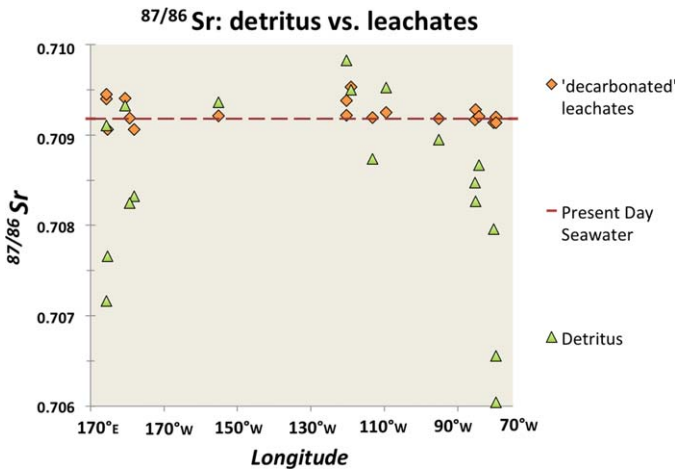

Figure 4. Sr isotope compositions of detritus and "decarbonated" leachates against longitude. The present-day seawater ratio is marked by the dashed line.

The $^{87}Sr/^{86}Sr$ ratios obtained for the 26 "decarbonated" leachates differ substantially from that of the detritus

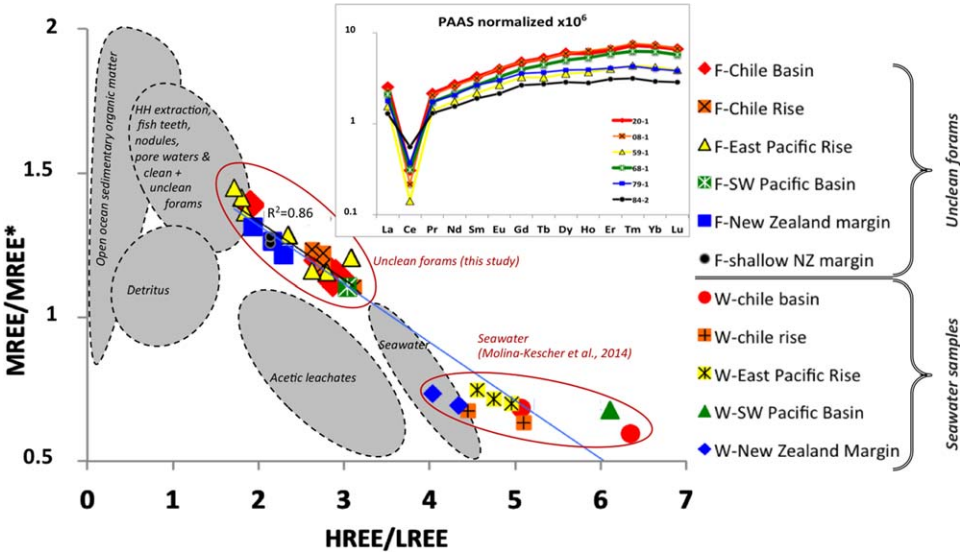

Figure 5. HREE/LREE (Tm+Yb+Lu/La+Pr+Nd) versus MREE/MREE* (Gd+Tb+Dy/LREE+HREE) of the REE concentrations normalized to Post-Achaean Australian Sedimentary Rocks (PAAS) [*Taylor and McLennan*, 1985] measured on "unclean" planktonic foraminifera samples of the different areas analyzed in this study (see legend: areas defined in Figure 3) and from seawater samples obtained for the same locations and depths [*Molina-Kescher et al*., 2014]. Shaded gray areas from *Martin et al*. [2010, and references therein], *Kraft et al*. [2013], and *Freslon et al*. [2014] are shown for comparison. PAAS normalized patterns from selected samples of each area are also presented in the smaller subplot.

(Figure 4) and average 0.70925 (±0.0003). This is close to the established seawater value of 0.70918 [e.g., *Henderson et al*., 1994] and thus apparently supports that the ε_{Nd} values obtained from the "decarbonated" leachates are entirely seawater derived. However, as discussed below in section 4.2.2 the interpretation is more complex.

3.3. Elemental Ratios and REE Concentrations of the "Unclean" Foraminifera

Al/Ca ratios and REE patterns were obtained on the dissolved "unclean" foraminifera in order to detect any potential detrital contributions to the authigenic bottom water ε_{Nd} signal recorded by the Fe-Mn coatings of the planktonic foraminifera shells.

Al/Ca ratios (Table 2) were below detection limit in 13 of 22 samples and below 100 μmol/mol in the rest of the samples except 84-2 and 85-1. Values above 100 μmol/mol have been considered to indicate clay contamination of the samples [*Ni et al*., 2007; *Kraft et al*., 2013]. Only samples 84-2 (362 μmol/mol) and 85-1 (229 μmol/mol), located very close to South Island of New Zealand on the Western Chatham Rise (Figure 1) show Al/Ca ratios above 100 μmol/mol indicating that the extracted Nd isotope ratios of these two samples might be slightly contaminated by the detrital Nd isotope composition (see section 4.2.1). The REE concentration patterns normalized to the Post Achaean Australian Sedimentary Rocks (PAAS) [*Taylor and McLennan*, 1985] (Table 3 and Figure 5) show seawater-like patterns for all unclean foraminifera samples, including a marked Ce anomaly and a progressive light to heavy increase in REE abundance, although the HREE enrichment is less pronounced than in seawater. The Ce anomaly is, however, less pronounced near the New Zealand Margin, such as in sample 84-2 (Table 3 and Figure 5). In Figure 5, the shape of the REE patterns of "unclean" foraminifera and seawater of this and other studies [e.g., *Martin et al*., 2010] is compared and suggests that detrital contributions do not affect the REE concentrations of the Fe-Mn coatings extracted from "unclean" foraminifera (R = 0.86). These data generally support the bottom seawater origin of the ε_{Nd} signatures obtained from "unclean" foraminifera shells, except for samples 84-2 and 85-1.

3.4. ^{14}C Ages of Core-Tops

The calibrated ^{14}C ages of the eight core-tops analyzed (Table 2) range between 4142 ± 259 and 24,226 ± 811 years, as a consequence of the very low sedimentation rates in the open South Pacific that range from less than 1 mm/kyr [*Glasby et al*., 2007] to 20 mm/kyr [*Tiedemann et al*., 2014]. Rates are considerably higher at around 138 mm/kyr on the New Zealand Margin [*Carter et al*., 1996], but the Bounty Trough

has lower sedimentation rates than other parts of this margin: 3–27 mm/kyr [*Griggs et al*., 1983]. This leads to core-tops with a mixed/average age as old as ~24 kyr before present (17-1) corresponding to the Last Glacial Maximum (LGM) and only two samples (20-1 and 84-2) with middle Holocene ages (4142 ± 259 and 4952 ± 238 years BP, respectively). All other analyzed samples represent the period of the last deglaciation and the early Holocene with an age range between ~8000 and ~17,000 years.

4. Discussion

4.1. Seawater-Sediment Interaction and the Present-Day Seawater Nd Isotope Signature

Direct comparison of bottom water ε_{Nd} signatures with those of the detrital material of our study allows an estimation of the importance of seawater-sediment interaction, a possible mechanism for boundary exchange [*Lacan and Jeandel*, 2005], for the seawater Nd cycle in the South Pacific. The New Zealand Margin (Figure 3a) is the area where the differences in ε_{Nd} signatures between seawater and detrital silicate are largest, reaching up to 6 ε_{Nd} units. Sediment samples 78-1 and 79-1 are of particular interest for this purpose given that they were obtained together with the overlying bottom water samples (MuC-78 and MuC-79) in the same multicorer tube. In a previous study, these water samples were found to be relatively unradiogenic at ε_{Nd} values of -9.0 ± 0.3 and -10.3 ± 0.3, which was attributed to admixed North Atlantic Deep Water (NADW) [*Molina-Kescher et al*., 2014]. This remnant of NADW has also been documented in this region based on elevated salinity and low nutrients [*Reid and Lynn*, 1971; *Warren*, 1973; *Gordon*, 1975] and was named *upper* Lower Circumpolar Deep Water (*u*LCDW), located between 2800 and 3900 m water depth [*Gordon*, 1975; *McCave et al*., 2008; *Noble et al*., 2013]. The large difference between the Nd isotope compositions of detrital silicates and seawater observed in our study indicates that sedimentary contributions do not play a significant role for setting the dissolved Nd isotope signature of the bottom waters of this region and confirms the advective origin of these relatively unradiogenic seawater signatures. This suggests the absence of seawater-sediment interaction "boundary exchange" in the Deep Western Boundary Current (DWBC) of the Southwest Pacific [*Molina-Kescher et al*., 2014], in contrast to the observations in the DWBC of the Southwestern Indian Ocean [*Wilson et al*., 2012]. Although the Nd isotope composition of bottom waters before entering the Bounty Trough is unknown and the large detrital-seawater ε_{Nd} difference itself does not completely exclude boundary exchange given that phases other than detrital silicates may be responsible for this process, the overall relatively radiogenic Nd isotope compositions of nearby continental rocks and sediments [e.g., *Jeandel et al*., 2007] of the area argue against this possibility. The absence of boundary exchange in the DWBC of the South Pacific may be explained by the low sedimentation rates in this area and the correspondingly longer periods of time in contact with seawater, which may have led to a loss of their reactivity.

The relatively unradiogenic residual ε_{Nd} signature of NADW observed on the southern flank of the Chatham Rise disappears quickly to the north of our sampling sites as documented by Holocene "unclean" planktonic foraminifera ε_{Nd} data of -6.8 ± 0.4 obtained at the northern flank of the Chatham Rise [*Noble et al*., 2013]. This suggests a clear separation of the hydrography on both sides of the rise in terms of dissolved Nd isotope compositions with a clear dominance of Pacific-derived waters on the northern flank of Chatham Rise, similar to observations based on hydrographic parameters [*McCave et al*., 2008; *Bostock et al*., 2011]. The difference may also be the result of a recent change in the circulation (see section 4.2.1). However, the absence of dissolved seawater ε_{Nd} measurements from the northern Chatham Rise does not allow verification of these hypotheses as yet and although boundary exchange [*Noble et al*., 2013] may be responsible for significant modifications of seawater ε_{Nd} signatures, clearly its absence in the Bounty Trough suggests these processes are spatially and temporally variable. This difference in seawater-sediment interaction in the eastern New Zealand Margin could result from differences in organic matter content of the sediments, which is considerably higher, of up to 14%, on the northern side of the Chatham Rise, whereas the southern side in the Bounty Trough values are between 1 and 3% [*Hayward et al*., 2002].

Sediments from other locations of this study, such as samples 68-1 (Figure 3b) or 63-1 and 64-2 (Figure 3c), show very similar detrital, authigenic, and seawater ε_{Nd} signatures, which suggests potential seawater-sediment interactions, potentially caused by labile Nd in detrital silicates. However, this is most likely coincidence, given that the seawater Nd isotope compositions of these locations are clearly consistent with the

hydrographic properties and water mass mixing [*Molina-Kescher et al*., 2014] while the detrital silicates show fully coherent combined Nd-Sr isotope signatures according to their provenance (see section 4.3.2).

Hydrothermal contributions to seawater Nd isotope compositions of the East Pacific Rise are also insignificant given that the highly radiogenic Nd contributions of MORB to the detrital fraction of sample 57-1 (see section 3.1) are not reflected in the corresponding seawater signatures of profiles 50 and 54 between 700 and 1900 m (Figure 3c).

4.2. Reliable Extraction of the Seawater Nd Isotope Signatures From the Sediments

One of the main goals of this study is a comparison of the results of the different methods to extract bottom water Nd isotope compositions to the signatures of the overlying water column and of the detrital fraction in order to identify the most appropriate technique for future paleoceanographic reconstructions of the deep water circulation in this area. This comparison, presented in Figure 3, shows that the reliability of the different methods changes considerably between locations, although "unclean" planktonic foraminifera, leachates, and fish teeth display ε_{Nd} values that are close to the respective seawater signatures and are therefore considered the best techniques. Although mostly yielding trends and changes with water depth similar to seawater ε_{Nd}, the results of all sediment extraction techniques applied here are offset to more radiogenic Nd isotope compositions and thus toward the compositions of the detrital material. It might be argued that the offset between sedimentary and seawater ε_{Nd} signatures is a consequence of partial dissolution of the detrital silicate fraction, which during the extraction procedures biased the extracted seawater Nd isotope compositions. As indicated by Al/Ca and REE patterns (see section 4.2.1), this is most probably the case for samples 84-2 and 85-1, and for the "decarbonated" leachates in near coastal areas (see sections 4.2.2 and 4.2.3) but cannot explain the foraminifera and fish teeth data. Therefore, this offset is most likely the result of the relatively old integrated age of the core-top sediments (see section 4.2.1).

The presence of basaltic material in the sediment of sample 57-1 on the East Pacific Rise (Figure 3c) is not reflected in the leached authigenic Nd isotope signatures of the same samples. This suggests an insignificant hydrothermal contribution to these sediments and documents that the seawater signature can be extracted reliably despite the presence of high reactive basaltic material [*Pearce et al*., 2013] in the sediments.

4.2.1. Integration of ε_{Nd} Values From Seawater Subject to Different Circulation States

The extremely low sedimentation rates in the South Pacific result in the integration of seawater ε_{Nd} values reflecting different circulation states of the past up to ~24,000 years. ^{230}Th analyses performed in the area of this study [*Schmitz et al*., 1986] found evidence of sediment redistribution processes in the western and central South Pacific, which have particularly affected the area near the Valerie Passage, where the DWBC intensifies [*Carter et al*., 1996]. This area is located much further north than the locations of our samples. Significant sediment redistribution processes have only been observed further south below the South Pacific sector of the Antarctic Circumpolar Current [*Chase et al*., 2003]. The low sedimentation rates observed in our entire study area essentially exclude any significant accumulation of sediments transported by bottom currents and winnowing would not affect the authigenic Nd isotope signatures. Therefore, the observed ε_{Nd} offsets between local seawater and biogenic/authigenic phases are very unlikely significantly influenced by sediment redistribution processes.

Al/Ca ratios and REE patterns (section 3.3) measured in "unclean" foraminifera in almost all cases clearly support a seawater origin of the ε_{Nd} signatures, which also supports the same origin for Nd extracted from the fish teeth and "nondecarbonated" leachates given that all three methods generally yield identical Nd isotope compositions within error. Bioturbation is most probably not the mechanism responsible for the integration of the ε_{Nd} signatures of different circulation modes in the authigenic phases as it varies with grain size [*Bard*, 2001] and consequently coarser fractions (forams/fish teeth) and finer fractions (leachates) should register different Nd isotope compositions, which is not the case. Therefore, the interaction of pore waters with the authigenic phases could play a crucial role in their ε_{Nd} signatures. However, Figure 5 shows that the PAAS-normalized REE concentration patterns of our "unclean" foraminifera are more similar to typical seawater than observed in other studies and closer to the seawater end-member in the MREE/MREE* versus HREE/LREE plot [*Martin et al*., 2010, and references therein; *Kraft et al*., 2013]. Authigenic sedimentary REE extractions usually present a characteristic middle REE enrichment ("MREE-bulge") as a consequence of diagenesis in suboxic and anoxic sediments that results in the reduction of Fe-Mn oxyhydroxides

[*Haley et al*., 2004; *Martin et al*., 2010, and references therein; *Kim et al*., 2012; *Kraft et al*., 2013] and/or the degradation of organic matter within the sediment [*Freslon et al*., 2014]. The lower MREE/MREE* ratios than observed in other studies (gray fields in Figure 5, obtained from *Martin et al*. [2010, and references therein]) suggests a lower pore water contribution than in other regions but all pore waters do not have high MREE/MREE* ratios [*Haley et al*., 2004], and without pore water measurements from this region no firm conclusion can be made. The relatively low MREE/MREE* ratios (Figure 5) may also reflect the low primary productivity in the oligotrophic waters between the South Pacific subtropical gyre and the subtropical front delivering little organic matter to the sediments.

The integration of signatures from different periods of time results in some important observations: in the case of the water and sediment samples simultaneously retrieved within the same multicore tube from the New Zealand margin (MuC-78, 78-1, and MuC-79, 79-1; Figure 3a), the relatively unradiogenic seawater ε_{Nd} signal (-9.0 and -10.3, respectively) does not match "unclean" foraminifera ε_{Nd} signatures (-7.3 ± 0.4 and -7.7 ± 0.4, respectively) but the latter agree with Holocene "unclean" foram data (-6.8 ± 0.4) from the northern flank of the Chatham Rise [*Noble et al*., 2013], obtained at 500–1000 km to the north of our location on similar depths ($\sim$3200 m; see Figure 1). This suggests that the remnant of NADW identified by the seawater Nd isotope composition (see section 4.1) only represents a "snapshot" of today's seawater composition, most probably caused by a recent change in the circulation of the area that has not yet been transferred to the sedimentary record. A similar observation was made in the eastern South Pacific in the vicinity of the Chile Rise (Figure 3d), where a remarkable offset between the integrated LGM-Holocene sedimentary ε_{Nd} signatures and the prevailing seawater Nd isotope compositions ($\sim$4 ε_{Nd} units) is found. This is considerably larger than the offsets between seawater and authigenic sediment fractions in the adjacent Chile Basin and East Pacific Rise areas (Figures 3c and 3e). Today the deeper part (below 2000 m water depth) of the Chile Rise area, between 90°W and 110°W, is occupied by CDW and thus relatively negative seawater Nd isotope compositions prevail compared to the adjacent regions, which are dominated by NPDW. A deepening of radiogenic NPDW during glacial periods, as already deduced in a number of paleoceanographic studies [e.g., *Matsumoto et al*., 2002, and references therein], would produce a more pronounced change of Nd isotope compositions in the less radiogenic waters of the Chile Rise area (Figure 3d) explaining the large seawater-sediment ε_{Nd} offset observed (Figure 3d).

4.2.2. Detrital Contributions

Although "unclean" foraminifera have generally proven to be reliable recorders of seawater Nd isotope compositions [e.g., *Roberts et al*., 2010; *Tachikawa et al*., 2014], in this study, the two samples from locations closest to land, namely 84-2 (995 m depth) and 85-1 (832 m depth), show relatively high Al/Ca ratios of 362 and 229 μmol/mol and high proportions of detrital silicate of 57% and 64%, respectively (Table 2). This indicates that the extracted Nd isotope signatures were slightly contaminated with detrital silicate. It is also possible that the partial dissolution of the mainly volcanogenic material during early diagenetic processes and subsequent incorporation of detrital Nd isotope compositions into Fe-Mn oxhydroxide coatings could drive ε_{Nd} signatures more radiogenic (-5.4 ± 0.3 and -5.8 ± 0.3, respectively) than expected for Antarctic Intermediate Water (AAIW) prevailing at the water depths of these two samples. Foraminiferal Nd isotope data obtained from settings close to the coast may generally be prone to such bias and therefore should be accompanied by elemental data to ensure that the removal of detrital material was sufficient. Similar observations have been made in other near coastal areas, such as the Gulf of Guinea [*Kraft et al*., 2013].

4.2.3. Failure of "Decarbonated" Leachates as Recorders of Seawater Nd Isotope Compositions in Volcanic Regions

A decarbonation step prior to the HH-leach of the bulk sediment has been a commonly used procedure of the seawater Nd isotope extraction methods for the reconstructions of past deep water circulation regimes [e.g., *Piotrowski et al*., 2005, 2008; *Gutjahr et al*, 2007, 2008]. In our study area, "decarbonated" leachates are, however, clearly biased toward detrital signatures in near coastal locations, such as the New Zealand Margin (Figure 3a) and the Chile Basin (Figure 3e). The ε_{Nd} signatures of the unclean forams and leachates are significantly different from the "decarbonated" leachates, with the latter in most cases being similar to or indistinguishable from the signatures of the detrital fraction. As shown by *Wilson et al*. [2013], the use of an acetic acid decarbonation step prior to the HH leach results in the partial dissolution of remaining nonauthigenic phases, in our case mostly of readily acid-soluble particles of volcanic origin, which alter the signatures extracted by "decarbonated" leaching. It is evident that this procedure fails to provide reliable bottom

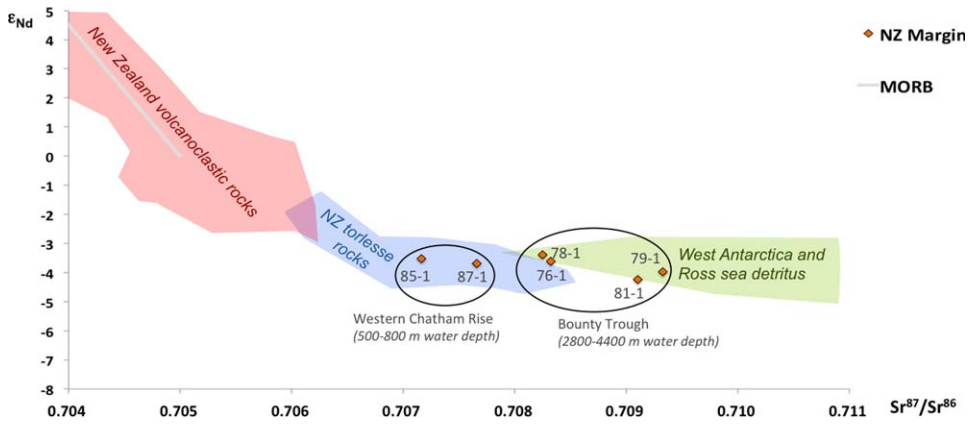

Figure 6. Combined Nd and Sr isotope signatures of detrital core-tops obtained on the New Zealand Margin (orange symbols; see locations in Figures 1 and 3a), which are subdivided into two groups as a function of distance to New Zealand (Western Chatham Rise < Bounty Trough), and their most probable sources represented by the colored areas: Volcanoclastic rocks, most representative of North Island (New Zealand) in red (data from *Wandres et al.* [2004] and *Adams et al.* [2005]); Torlesse metasedimentary rocks, dominant in South Island (New Zealand) in blue [*Wandres et al.*, 2004; *Adams et al.*, 2005]; and detrital surface sediments from offshore West Antarctica and the Ross sea (combined from *Roy et al.* [2007] and *Hemming et al.* [2007]).

water ε_{Nd} signatures in near coastal regions of the South Pacific, whereas at the open ocean sites the results of all extraction methods applied, including "decarbonated" leaching, are identical within error and are thus considered reliable. This complements results from the North Atlantic [*Elmore et al.*, 2011], where "decarbonated" leaching failed to produce the seawater Nd isotope composition near active volcanic settings such as Iceland. On the other hand, "decarbonated" leaching has been shown to be a reliable technique in other open ocean regions such as the Western North Atlantic [*Gutjahr et al.*, 2008], the Indian Ocean [*Piotrowski et al.*, 2009], or the Atlantic sector of the Southern Ocean [*Piotrowski et al.*, 2005, 2012; *Gutjahr et al.*, 2007] among other regions. The success of this technique may therefore be related to the absence of active volcanism in the studied area. This technique has also failed in regions of high detrital sedimentation rates where the presence of "preformed" continental oxides may contaminate the seawater signal extracted by leaching [e.g., *Bayon et al.*, 2004; *Kraft et al.*, 2013], which may also be the case for the samples from the New Zealand Margin. As shown in section 3.2 and Figure 4, obtaining a Sr isotope signature close to that of modern seawater in the "decarbonated" leachates may not serve as an unambiguous proof for a pure seawater Nd isotope signature. In samples rich in carbonates with relatively high Sr concentrations, even a small fraction of residual carbonate after the acetic acid treatment may lead to a dominance of the seawater Sr isotope signature in the HH leach.

4.3. Provenance of Detrital Material in the South Pacific Deduced From Nd-Sr Isotope Compositions

The clear general trend to more positive (negative) Nd (Sr) isotope signatures of the detritus at the ocean margins shown in Figure 2 demonstrates the importance of the erosion of young volcanogenic material from South America and New Zealand. Figures 6 and 7 compare combined Nd and Sr isotope compositions of the detrital silicate samples of this study (symbols) with those of the lithologies and fine particles from the surrounding landmasses, which are the most likely source regions of the weathered terrigenous material supplied to the South Pacific (shaded areas).

4.3.1. New Zealand Margin

Figure 6 compares the isotopic compositions of the samples obtained from the New Zealand Margin sediments (orange diamonds) with the lithologies of the two dominant rock types of these islands: volcanoclastic rocks predominant in North Island (red), where active volcanic regions such as the Taupo Volcanic Zone are present and therefore similar in isotope composition to MORB; and Torelesse Terrane metasediment (blue), a dominant New Zealand sedimentary sequence that dominates the eastern flank of New Zealand's Alps of the South Island [*Adams et al.*, 2005]. Combined Nd and Sr isotope compositions of detrital silicates of West Antarctica and Ross sea sediments are also shown (green).

We observe essentially the same Nd isotope compositions for all detrital samples in this area, whereas the $^{87}Sr/^{86}Sr$ ratios vary between 0.7072 and 0.7093. The samples obtained at Western Chatham Rise, 87-1 and

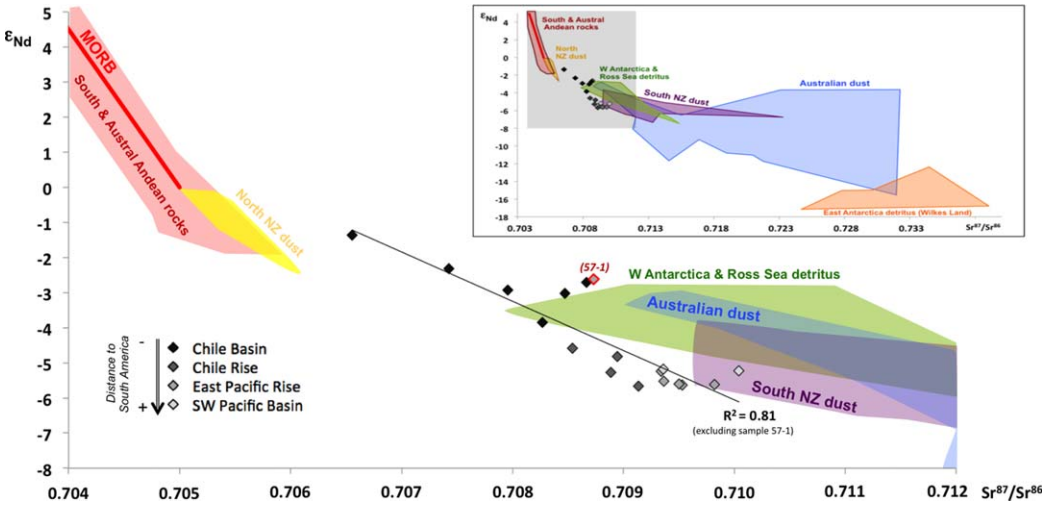

Figure 7. Combined Nd and Sr isotope signatures of detrital core-tops from the open South Pacific (diamonds) grouped by areas (as defined in Figure 3) and coded in black to light gray tones as a function to the distance to South America (see legend in the figure). The most probable sources that surround the South Pacific are presented as colored Sr-Nd areas: the Southern [*Hickey et al*., 1986; *Futa and Stern*, 1988] and Austral Andes [*Futa and Stern*, 1988; *Stern and Kilian*, 1996] combined, in red. Fine-grained particles (<5 μm) susceptible to be transported by wind from: North Island (New Zealand) in yellow (data from *Delmonte et al*. [2004]); South Island (New Zealand) in purple [*Taylor et al*., 1983; *Delmonte et al*., 2004]; and Eastern Australia in blue [*Revel-Rolland et al*., 2006]. Circumantarctic surface sediments (detritus) from Wilkes Land, in orange; and West Antarctica and Ross Sea, in green (combined from *Roy et al*. [2007] and *Hemming et al*. [2007]). Note that the smaller subplot shows a larger Nd-Sr area. The gray square is shown in detail in the large plot.

85-1, are the shallowest (542 and 842 m) and closest to the South Island (~200 km from the coast). These samples clearly overlap with the lithological range of the Torelesse rocks of the eastern New Zealand Alps, which is the source region for the weathered material to the entire Bounty Trough sedimentary system [*Carter and Carter*, 1996]. The volcanic material from the North Island apparently does not reach our study area.

Samples 76-1, 78-1, 79-1, and 81-1, obtained in the Bounty Trough between 500 and 850 km off the coast from water depths between ~2800 and ~4400 m, show higher $^{87}Sr/^{86}Sr$ ratios than the sediments from the Western Chatham Rise and their expected source (eastern NZ Alps). This most probably indicates a fractionation of Sr isotopes due to grain size effects [*Innocent et al*., 2000; *Tütken et al*., 2002], which has been shown to result in more radiogenic Sr^{87}/Sr^{86} ratios as particle grain size decreases. This is consistent with the fact that these locations are most distant from the coast and are the deepest samples, which are expected to be primarily composed of finer particles due to longer transport. These four samples show similar bulk detrital Sr isotope composition to samples obtained from the northern flank of the Chatham Rise [*Graham et al*., 1997; *Noble et al*., 2013] characterized by Sr^{87}/Sr^{86} ratios > 0.709. Variations in the source provenance, which seems less probable due to the short distance to New Zealand, could also explain the mismatch between New Zealand's Torelesse rocks and samples 76-1, 78-1, 79-1, and 81-1. The similarity of the isotopic composition of these samples to circum-Antarctic detritus may suggest that a part of the detrital silicates that reaches the Bounty Trough may originate from Antarctica and has been transported in suspension in circumpolar waters and the DWBC. Where this current originates, south of the Bounty Trough, it initially decelerates because of its loss of momentum when it detaches from the ACC [*Carter et al*., 1996]. This effect could be the cause for the settling of the transported fine particles. A similar mechanism has also been invoked for sediments in the Atlantic sector of the Southern Ocean [*Franzese et al*., 2006].

4.3.2. Open South Pacific

Figure 7 shows the Nd-Sr isotope compositions of the detrital silicate samples of this study (diamonds), excluding the samples from the New Zealand Margin (shown in Figure 6), and that of material that is likely to reach the South Pacific. These are the lithologies of the southern and austral Andes (red field), which will play an important role for the Chile Basin; dust and fine particles from Australia and New Zealand's North and South Islands (blue, yellow, and purple fields, respectively) brought by the dominant westerlies; and circum-Antarctic detritus to the south and southwest of the study area (West Antarctica, Ross Sea, and Wilkes Land; green and orange fields), from where the dominant oceanic currents may have transported this Antarctic lithogenic-derived material.

Long-distance transport from the continental sources allows only very fine-grained particles to reach these distal locations and therefore provenance rather than grain size has apparently been the most important factor controlling the Sr isotope composition of the detrital material in this area. This is also demonstrated by the significant correlation with the Nd isotope compositions of $R^2 = 0.81$ (excluding sample 57-1, clearly affected by MORB contributions (see section 3.1)). This correlation is geographically consistent given that ε_{Nd} signatures ($^{87}Sr/^{86}Sr$ ratios) generally decrease (increase) from near South American sites toward the open ocean: Chile Basin $>(<)$ Chile Rise $>(<)$ EPR and SWP, confirming the Andes as one of the source end-members. Fine-grain dust from North Island (New Zealand) also falls in the same field as Andean rocks because of its mainly volcanic origin, but it seems less probable that its presence in the detritus increases with distance from New Zealand. Furthermore, the North Island is not under the direct influence of the westerlies as it extends into the subtropical ridge of high pressure [*Delmonte et al*., 2004] and therefore it is likely only a minor source region of detritus to the eastern South Pacific.

Besides the south and Austral Andes, a second and robust end-member cannot be clearly deduced from Figure 7 as circum-Antarctic detritus and eolian dust from Australia and South Island (NZ) display similar Sr-Nd fields. Nevertheless, almost all samples follow a trend that clearly diverges from the West Antarctica and Ross Sea detritus, except for a few samples from the Chile Basin, which may indeed have been influenced by Antarctic-derived material transported to this location by surface currents such as the Humboldt Current. Whereas, we cannot completely exclude a contribution of Sr and Nd originating from residual coatings, this is not likely in view of the efficiency of the applied leaching procedures. The apparent bowing of the mixing line is most likely simply caused by a lack of combined Sr and Nd isotope data in the Sr isotope range between 0.705 and 0.708.

Therefore, the main source candidates for the detritus arriving in the South Pacific remain Australian and South Island (NZ) dust, as suggested by other authors before [e.g., *Rea*, 1994; *Stacin et al*., 2008]. The large arid continent of Australia, the eastern part of which is affected by the westerlies that move toward the South Pacific [e.g., *Leinen et al*., 1986; *Hesse*, 1994], has been even considered as the greatest contributor to atmospheric dust in the Southern Hemisphere [*Tanaka and Chiba*, 2006]. Central and east Australia present a huge variety of lithologies and therefore also display a large Nd-Sr field; nevertheless, the main area providing dust to the South Pacific are the Lake Eyre and Murray River Basins [*McTainsh*, 1989; *McGowan and Clark*, 2008; *Albani et al*., 2012], the Nd-Sr isotope composition of which ranges between -3 and -8 and 0.7090 and 0.7019, respectively [*Revel-Rolland et al*., 2006].

On the other hand, eastern South Island (NZ), although being smaller and wetter, also represents a major dust source to the South Pacific because of its proximity and because it has large loess deposits [*Berger et al*., 2002; *Eden and Hammond*, 2003] susceptible to transport by wind, especially during glacial periods when a large part of the New Zealand continental shelf was exposed. During the glacial period the dust deposition in the Pacific sector of the Southern Ocean was higher [e.g., *Lamy et al*., 2014] and as a consequence of the low sedimentation rates in our study area (see section 3.4) significant amounts of southern New Zealand glacial-detritus probably reached our study sites.

In summary, both South Island (NZ) and southeastern Australia probably contribute similar amounts of dust [see also *Stancin et al*., 2008] and can be considered the major sources of detrital silicates found in the SW Pacific Basin and Chile Rise near 45°S, confirming the absolute predominance of these dust sources until at least ~110°W in this latitude [*McGowan and Clark*, 2008; *Albani et al*., 2012]. In contrast, east of this longitude, the influence of these two sources in the detritus decreases, especially in the Chile Basin, where South American material contributes significantly, potentially also receiving supplies from the Antarctic.

5. Conclusions

The results of this study suggest that seawater-sediment interaction "boundary exchange" does not play a significant role for the Nd isotope composition of bottom waters of the western South Pacific. No alteration of the bottom waters could be found by comparing the core-top detrital silicate signature with the directly overlying seawater value [*Molina-Kescher et al*., 2014] at the Bounty Trough off New Zealand. At this continental margin location, dominated by terrigenous input, this probably results from a combination of the low sedimentation rates and low organic matter content causing low reactivity of the detrital silicate fraction in the area of rapid bottom water flow.

We compared authigenic and detrital core-top ε_{Nd} signatures to those of bottom waters in order to identify the most reliable method to extract seawater Nd signatures from South Pacific sediments. Authigenic seawater signatures extracted from "unclean" planktonic foraminifera; fossil fish teeth and "nondecarbonated" leachates are offset to more radiogenic values from seawater ε_{Nd} signatures. Independent evidence, such as REE patterns and Al/Ca measurements on "unclean" foraminifera indicate, however, that these three extraction methods effectively record bottom seawater signatures. We suggest that the observed offset between sediment and seawater Nd isotope compositions originates from the low sedimentation rates observed in this area, confirmed by ^{14}C ages of up to 24 kyr. Thus, the authigenic ε_{Nd} signature obtained from the core-top sediments integrates the Nd isotope signal of the Holocene and the last glacial to differing extents.

Detrital Nd and Sr isotopes indicate that the dominant sources of terrigenous material reaching the South Pacific between 35°S and 50°S are southeastern Australia and the South Island of New Zealand, the fine-grained material of which is transported by the dominant Westerlies. The influence of these two sources decreases toward the east, especially in the Chile Basin, where the detritus contains increased amounts of weathered material from the Southern and Austral Andes. Antarctica may also be a contributing source to the deposited lithogenic material of the South Pacific, especially in the domains of the Deep Western Boundary Current and the Humboldt Current.

Acknowledgments
We would like to thank the "Bundesministerium für Bildung und Forschung, Germany" for funding this project (03G0213B) as well as the crew members and participants of expedition SO213, in particular D. Nürnberg, R. Tiedemann, and F. Lamy for organizing and leading the cruise, which was part of the collaborative SOPATRA (SOuth PAcific paleoceanographic TRAnsect) project between the GEOMAR Helmholtz Centre for Ocean Research Kiel and the Alfred Wegener Institute for Polar and Marine Research (AWI) in Bremerhaven. D. Nürnberg and R. Tapia provided the ^{14}C dating and % weight data. We also want to thank C. Basak and E. E. Martin for helping with the identification of the fish teeth, J. Heinze for laboratory assistance and Derek Vance for the edition of this paper. Comments by A. Piotrowski, G. Bayon, N. Fagel, and an anonymous reviewer improved the quality of this paper significantly. All the results presented in this study are available in the database of PANGAEA® (www.pangaea.de).

References

Adams, C. J., R. J. Pankhurst, R. Maas, and I. L. Millar (2005), Nd and Sr isotopic signatures of metasedimentary rocks around the South Pacific margin and implications for provenance, *Geol. Soc. Spec. Publ.*, *246*, 113–141.

Albani, S., N. Mahowald, B. Delmonte, V. Maggi, and G. Winckler (2012), Comparing modeled and observed changes in mineral dust transport and deposition to Antarctica between the last glacial maximum and current climates, *Clim. Dyn.*, *38*, 1731–1755.

Arsouze, T., J. C. Dutay, F. Lacan, and C. Jeandel (2009), Reconstructing the Nd oceanic cycle using a coupled dynamical–biogeochemical model, *Biogeosciences*, *6*, 2829–2846.

Asahara, Y., F. Takeuchi, K. Nagashima, N. Harada, K. Yamamoto, K. Oguri, and O. Tadai (2012), Provenance of terrigenous detritus of the surface sediments in the Bering and Chukchi seas as derived from Sr and Nd isotopes: Implications for recent climate change in the Arctic regions, *Deep Sea Res., Part II*, *61–64*, 155–171.

Bard, E. (1988), Correction of accelerator mass spectrometry 14C ages measured in planktonic foraminifera: Paleoceanographic implications, *Paleoceanography*, *3*(6), 635–645, doi:10.1029/PA003i006p00635.

Bard, E. (2001), Paleoceanographic implications of the difference in deep-sea sediment mixing between large and fine particles, *Paleoceanography*, *16*(3), 235–239.

Barrat, J. A., F. Keller, J. Amossé, R. N. Taylor, R. W. Nesbitt, and T. Hirata (1996), Determination of rare earth elements in sixteen silicate reference samples by ICP-MS after Tm addition and ion exchange separation, *Geostand. Geoanal. Res.*, *20*, 133–139.

Basak, C., E. E. Martin, K. Horikawa, and T. M. Marchitto (2010), Southern Ocean source of 14C-depleted carbon in the North Pacific Ocean during the last deglaciation, *Nat. Geosci.*, *3*(11), 770–773.

Bayon, G., C. R. German, R. M. Boella, J. A. Milton, R. N. Taylor, and R. W. Nesbitt (2002), An improved method for extracting marine sediment fractions and its application to Sr and Nd isotopic analysis, *Chem. Geol.*, *187*, 179–199, doi:10.1016/s0009-2541(01)00416-8.

Berger, G. W., B. J. Pillans, J. G. Bruce, and P. D. McIntosh (2002), Luminescence chronology of loess–paleosol sequences from southern South Island, New Zealand, *Quat. Sci. Rev.*, *21*, 1899–1913.

Bostock, H. C., B. W. Hayward, H. L. Neil, K. I. Currie, and G. B. Dunbar (2011), Deep-water carbonate concentrations in the southwest Pacific, *Deep Sea Res., Part I*, *58*, 72–85.

Carter, L., R. M. Carter, I. N. McCave, and J. Gamble (1996), Regional sediment recycling in the abyssal Southwest Pacific Ocean, *Geology*, *24*, 735–738.

Carter, P., D. Vance, C. D. Hillenbrand, J. A. Smith, and D. R. Shoosmith (2012), The neodymium isotopic composition of waters masses in the eastern Pacific sector of the Southern Ocean, *Geochim. Cosmochim. Acta*, *79*, 41–59.

Carter, R. M., and L. Carter (1996), The abyssal Bounty Fan and lower Bounty Channel: Evolution of a rifted-margin sedimentary system, *Mar. Geol.*, *130*, 181–202.

Charbonnier, G., et al. (2012), Reconstruction of the Nd isotope composition of seawater on epicontinental seas: Testing the potential of Fe-Mn oxyhydroxide coatings on foraminifera test for deep-time investigations, *Geochim. Cosmochim. Acta*, *99*, 39–56.

Chase, Z., R. F. Anderson, M. Q. Fleisher, and P. W. Kubik (2003), Accumulation of biogenic and lithogenic material in the Pacific sector of the Southern Ocean during the past 40,000 years, *Deep Sea Res., Part II*, *50*, 799–832.

Clague, D. A., J. B. Paduan, and A. S. Davis (2009), Widespread strombolian eruptions of mid ocean ridge basalt, *J. Volcanol. Geotherm. Res.*, *180*(2–4), 171–188, doi:10.1016/j.jvolgeores.2008.08.007.

Delmonte, B., I. Basile-Doelsch, J.-R. Petit, V. Maggi, M. Revel-Rolland, A. Michard, E. Jagoutz, and F. Grousset (2004), Comparing the Epica and Vostok dust records during the last 220,000 years: Stratigraphical correlation and provenance in glacial periods, *Earth Sci. Rev.*, *66*, 63–87.

Dou, Y., S. Yang, Z. Liu, X. Shi, J. Li, H. Yu, and S. Berne (2012), Sr-Nd isotopic constrains on terrigenous sediment provenances and Kuroshio Current variabilita in the Okinawa Trough during the late Quaternary, *Palaeogeogr. Palaeoclimatol. Palaeoecol.*, *356–366*, 38–47.

Eden, D. N., and A. P. Hammond (2003), Dust accumulation in the New Zealand region since the last glacial maximum, *Quat. Sci. Rev.*, *22*, 2037–2052.

Ehlert, C., M. Frank, B. A. Haley, U. Böniger, P. De Deckker, and F. X. Gingele (2011), Current transport versus continental inputs in the eastern Indian Ocean: Radiogenic isotope signatures of clay size sediments, *Geochem. Geophys. Geosyst.*, *12*, Q06017, doi:10.1029/2011GC003544.

Elderfield, H., P. Ferretti, M. Greaves, S. Crowhurst, I. N. McCave, D. Hodell, and A. M. Piotrowski (2012), Evolution of ocean temperature and ice volume through the mid-Pleistocene climate transition, *Science*, *337*(6095), 704–709.

Elmore, A. C., A. M. Piotrowski, J. D. Wright, and A. E. Scrivner (2011), Testing the extraction of past seawater Nd isotopic composition from North Atlantic marine sediments, *Geochem. Geophys. Geosyst.*, *12*, Q09008, doi:1029/02011GC003741.
Fagel, N., and N. Mattielli (2011), Holocene evolution of deep circulation in the northern North Atlantic traced by Sm, Nd and Pb isotopes and bulk sediment mineralogy, *Paleoceanography*, *26*, PA4220, doi:10.1029/2011PA002168.
Fletcher, M.-S., and P. I. Moreno (2012), Have the Southern Westerlies changed in a zonally symmetric manner over the last 14,000 years? A hemisphere-wide take on a controversial problem, *Quat. Int.*, *253*, 32–46.
Frank, M. (2002), Radiogenic isotopes: Tracers of past ocean circulation and erosional input, *Rev. Geophys.*, *40*(1), 1001, doi:10.1029/2000RG000094.
Franzese, A. M., S. R. Hemming, S. L. Goldstein, and R. F. Anderson (2006), Reduced Agulhas leakage at the LGM inferred from an integrated provenance and flux study, *Earth Planet. Sci. Lett.*, *250*, 72–88.
Freslon, N., et al. (2014), Rare earth elements and neodymium isotopes in sedimentary organic matter, *Geochim. Cosmochim. Acta*, *140*, 177–198.
Futa, K., and C. R. Stern (1988), Sr and Nd isotopic and trace element compositions of Quaternary volcanic centers of the southern Andes, *Earth Planet. Sci. Lett.*, *88*, 253–262.
Glasby, G. P. (1991), Mineralogy, geochemistry, and origin of Pacific red clays: A review, *N. Z. J. Geol. Geophys.*, *34*, 167–176.
Glasby, G. P. (2007), Broad region of no sediment in the Southwest Pacific Basin: Comment and reply: Comment, *Geology*, *35*, e132, doi: 10.1130/G23843C.1.
Goldstein, S. L., and S. R. Hemming (2003), Long lived isotopic tracers in oceanography, paleoceanography and ice-sheet dynamics, in *Treatise Geochemistry*, vol. 6.17, pp. 453–489, Elsevier, N. Y.
Goldstein, S. L., R. K. O'Nions, and P. J. Hamilton (1984), A Sm-Nd isotopic study of atmospheric dusts and particulates from major river systems, *Earth Planet. Sci. Lett.*, *70*, 221–236, doi:10.1016/0012-821X(84)90007-4.
Gordon, A. L. (1975), An Antarctic oceanographic section along 170°E, *Deep Sea Res. Oceanogr. Abstr., Part II*, *22*, 357–377.
Graham, I. J., G. P. Glasby, and G. J. Churchman (1997), Provenance of the detrital component of deep-sea sediments from the SW Pacific Ocean based on mineralogy, geochemistry and isotopic composition, *Mar. Geol.*, *140*, 75–96.
Greaves, M. J., P. J. Statham, and H. Elderfield (1994), Rare earth element mobilization from marine atmospheric dust into seawater, *Mar. Chem.*, *46*, 255–260.
Griggs, G. B., L. Carter, J. P. Kennett, and R. M. Carter (1983), Late Quaternary marine stratigraphy southeast of New Zealand, *Geol. Soc. Am. Bull.*, *94*, 791–797.
Grousset, F., and P. Biscaye (2005), Tracing dust sources and transport patterns using Sr, Nd and Pb isotopes, *Chem. Geol.*, *222*, 149–167.
Gutjahr, M., M. Frank, C. H. Stirling, V. Klemm, T. van de Flierdt, and A. N. Halliday (2007), Reliable extraction of a deepwater trace metal isotope signal from Fe-Mn oxyhydroxide coatings of marine sediments, *Chem. Geol.*, *242*, 351–370, doi:10.1016/j.chemgeo.2007.03.021.
Gutjahr, M., M. Frank, C. H. Stirling, L. D. Keigwin, and A. N. Halliday (2008), Tracing the Nd isotope evolution of North Atlantic deep and intermediate waters in the western North Atlantic since the Last Glacial Maximum from Blake Ridge sediments, *Earth Planet. Sci. Lett.*, *266*, 61–77, doi:10.1016/j.epsl.2007.10.037.
Haley, B. A., G. P. Klinkhammer, and J. McManus (2004), Rare earth elements in pore waters of marine sediments, *Geochim. Cosmochim. Acta*, *68*, 1265–1279.
Hathorne, E. C., B. A. Haley, T. Stichel, P. Grasse, M. Zieringer, and M. Frank (2012), Online preconcentration ICP-MS analysis of rare earth elements in seawater, *Geochem. Geophys. Geosyst.*, *13*, Q01020, doi:10.1029/2011GC003907.
Hayward, B. W., H. Neil, R. Carter, H. R. Grenfell, and J. J. Hayward (2002), Factors influencing the distribution patterns of recent deep-sea benthic foraminifera, east of New Zealand, Southwest Pacific Ocean, *Mar. Micropaleontol.*, *46*, 139–176.
Helo, C., M.-A. Longpré, N. Shimizu, D. A. Clague, and J. Stix (2011), Explosive eruptions at mid-ocean ridges driven by CO_2-rich magmas, *Nat. Geosci.*, *4*, 260–263, doi:10.1038/ngeo1104.
Hemming, S. R., T. van der Flierdt, S. L. Goldstein, A. M. Franzese, M. Roy, G. Gastineu, and G. Landrot (2007), Strontium isotope tracing of terrigenous sediment dispersal in the Antarctic Circumpolar Current: Implications for constraining frontal positions, *Geochem. Geophys. Geosyst.*, *8*, Q06N13, doi:10.1029/2006GC001441.
Henderson, G. M., D. J. Martel, R. K. O'Nions, and N. J. Shackleton (1994), Evolution of seawater $^{87}Sr/^{86}Sr$ over the last 400 ka: The absence of glacial/interglacial cycles, *Earth Planet. Sci. Lett.*, *128*, 643–651, doi:10.1016/0012-821X(94)90176-7.
Hesse, P. P. (1994), The record of continental dust from Australia in Tasman Sea sediments, *Quat. Sci. Rev.*, *13*, 257–272.
Hickey, R. L., F. A. Frey, and D. C. Gerlach (1986), Multiple sources for basaltic arc rocks from the southern volcanic zone of the Andes (34°-41°S): Trace element and isotopic evidence for contributions from subducted oceanic crust, mantle and continental crust, *J. Geophys. Res.*, *91*, 5963–5983.
Horwitz, E. P., R. Chiarizia, and M. L. Dietz (1992), A novel strontium-selective extraction chromatographic resin, *Solvent Extraction Ion Exch.*, *10*, 313–336, doi:10.1080/07366299208918107.
Huang, K.-F., D. W. Oppo, and W. B. Curry (2014), Decreased influence of Antarctic intermediate water in the tropical Atlantic during North Atlantic cold events, *Earth Planet. Sci. Lett.*, *384*, 200–208.
Innocent, C., N. Fagel, and R. Stevenson (1999), Do leaching experiments affect the Sm-Nd signature of deep-sea sediments? The example of the northern North Atlantic, *Can. J. Soil Sci.*, *79*, 707–713.
Innocent, C., N. Fagel, and C. Hillaire-Marcel (2000), Sm-Nd isotope systematics in deep-sea sediments: Clay-size versus coarser fractions, *Mar. Geol.*, *168*, 79–87.
Jacobsen, S. B., and G. J. Wasserburg (1980), Sm-Nd isotopic evolution of chondrites, *Earth Planet. Sci. Lett.*, *50*, 139–155.
Jeandel, C., T. Arsouze, F. Lacan, P. Techine, and J. C. Dutay (2007), Isotopic Nd compositions and concentrations of the lithogenic inputs into the ocean: A compilation, with an emphasis on the margins, *Chem. Geol.*, *239*, 156–164.
Jeandel, C., H. Delattre, M. Grenier, C. Pradoux, and F. Lacan (2013), Rare earth element concentrations and Nd isotopes in the Southeast Pacific Ocean, *Geochem. Geophys. Geosyst.*, *14*, 328–341, doi:10.1029/GC004309.
Jones, K. M., S. P. Khatiwala, S. L. Goldstein, S. R. Hemming, and T. van de Flierdt (2008), Modeling the distribution of Nd isotopes in the oceans using an ocean general circulation model, *Earth Planet. Sci. Lett.*, *272*(3–4), 610–619.
Kawabe, M., and S. Fujio (2010), Pacific Ocean circulation based on observation, *J. Oceanogr.*, *66*, 389–403.
Kim, J.-H., M. E. Torres, B. A. Haley, M. Kastner, J. W. Pohlman, M. Riedel, and Y.-J. Lee (2012), The effect of diagenesis and fluid migration on rare earth element distribution in pore fluids of the Northern Cascadia accretionary margin, *Chem. Geol.*, *291*, 152–165.
Klevenz, V., D. Vance, D. N. Schmidt, and K. Mezger (2008), Neodymium isotopes in benthic foraminifera: Core-top systematics and a down-core record from the Neogene south Atlantic, *Earth Planet. Sci. Lett.*, *265*, 571–587, doi:10.1016/j.epsl.2007.10.053.
Kraft, S., M. Frank, E. C. Hathorne, and S. Weldeab (2013), Assessment of seawater Nd isotope signatures extracted from foraminiferal shells and authigenic phases of Gulf of Guinea sediments, *Geochim. Cosmochim. Acta*, *121*, 414–435.

Lacan, F., and C. Jeandel (2005), Neodymium isotopes as a new tool for quantifying exchange fluxes at the continent-ocean interface, *Earth Planet. Sci. Lett.*, *232*, 245–257.
Lamy, F., R. Gersonde, G. Winckler, O. Esper, A. Jaeschke, G. Kuhn, J. Ullermann, A. Martinez-Garcia, F. Lambert, and R. Kilian (2014), Increased dust deposition in the Pacific Southern Ocean during glacial periods, *Science*, *343*, 403–407, doi:10.1126/science.1245424.
Le Fevre, B., and C. Pin (2005), A straightforward separation scheme for concomitant Lu–Hf and Sm–Nd isotope ratio and isotope dilution analysis, *Anal. Chim. Acta*, *543*, 209–221.
Leinen, M., D. Cwienk, G. R. Heath, P. E. Biscay, V. Kolla, J. Thiede, and J. Pl. Dauphin (1986), Distribution of biogenic silica and quartz in recent deep-sea sediments, *Geology*, *14*, 199–203.
Martin, E. E., and B. A. Haley (2000), Fossil fish teeth as proxies for sea water Sr and Nd isotopes, *Geochim. Cosmochim. Acta*, *64*, 835–847, doi:10.1016/S0016-7037(99)00376-2.
Martin, E. E., and H. D. Scher (2004), Preservation of seawater Sr and Nd isotopes in fossil fish teeth: Bad news and good news, *Earth Planet. Sci. Lett.*, *220*, 25–39.
Martin, E. E., S. W. Blair, G. D. Kamenov, H. D. Scher, E. Bourbon, C. Basak, and D. N. Newkirk (2010), Extraction of Nd isotopes from bulk deep sea sediments for paleoceanographic studies on Cenozoic time scales, *Chem. Geol.*, *269*, 414–431, doi:10.1016/j.chemgeo.2009.10.016.
Martin, E. E., K. G. MacLeod, A. J. Berrocoso, and E. Bourbon (2012), Water mass circulation on Demerara Rise during the late Cretaceous based on Nd isotopes, *Earth Planet. Sci. Lett.*, *327–328*, 111–120.
Marx, S. K., K. S. Lavin, K. J. Hageman, B. S. Kamber, T. O'Loingsigh, and G. H. McTainsh (2014), Trace elements and metal pollution in aerosols at an alpine site, New Zealand: Sources, concentrations and implications, *Atmos. Environ.*, *82*, 206–217.
Matsumoto, K., T. Oba, J. Lynch-Stieglitz, and H. Yamamoto (2002), Interior hydrography and circulation of the glacial Pacific Ocean, *Quat. Sci. Rev.*, *21*, 1693–1704.
McCave, I. N., L. Carter, and I. R. Hall (2008), Glacial–interglacial changes in water mass structure and flow in the SW Pacific Ocean, *Quat. Sci. Rev.*, *27*, 1886–1908, doi:10.1016/j.quascirev.2008.07.010.
McGowan, H., and A. Clark (2008), Identification of dust transport pathways from Lake Eyre, Australia using Hysplit, *Atmos. Environ.*, *42*, 6915–6925.
McTainsh, G. H. (1989), Quaternary aeolian dust processes and sediments in the Australian region, *Quat. Sci. Rev.*, *8*, 235–253.
Molina-Kescher, M., M. Frank, and E. Hathorne (2014), South Pacific dissolved Nd isotope compositions and rare earth element distributions: Water mass mixing versus biogeochemical cycling, *Geochim. Cosmochim. Acta*, *127*, 171–189.
Ni, Y. Y., G. L. Foster, T. Bailey, T. Elliott, D. N. Schmidt, P. Pearson, B. Haley, and C. Coath (2007), A core top assessment of proxies for the ocean carbonate system in surface-dwelling foraminifers, *Paleoceanography*, *22*, PA3212, doi:10.1029/2006PA001337.
Noble, T. L., et al. (2012), Greater supply of Patagonian sourced detritus and transport by the ACC to the Atlantic sector of the Southern Ocean during the last glacial period, *Earth Planet. Sci. Lett.*, *317*, 374–385.
Noble, T. L., A. M. Piotrowski, and I. N. McCave (2013), Neodymium isotopic composition of intermediate and deep waters in the glacial southwest Pacific, *Earth Planet. Sci. Lett.*, *384*, 27–36.
Pahnke, K., S. L. Goldstein, and S. R. Hemming (2008), Abrupt changes in Antarctic intermediate water circulation over the past 25,000 years, *Nat. Geosci.*, *1*, 870–874, doi:10.1038/ngeo360.
Palmer, M. R., and H. Elderfield (1985), Variations in the Nd isotopic composition of foraminiferal from Atlantic Ocean sediments, *Earth Planet. Sci. Lett.*, *73*, 299–305, doi:10.1016/0012-821X(85)90078-0.
Palmer, M. R., and H. Elderfield (1986), Rare earth elements and neodymium isotopes in ferromanganese oxide coatings of Cenozoic foraminifera from the Atlantic Ocean, *Geochim. Cosmochim. Acta*, *50*, 409–417, doi:10.1016/0016-7037(86)90194-8.
Pearce, C. R., M. T. Jones, E. H. Oelkers, C. Pradoux, and C. Jeandel (2013), The effect of particulate dissolution on the neodymium (Nd) isotope and rare earth element (REE) composition of seawater, *Earth Planet. Sci. Lett.*, *369–370*, 21–40.
Pena, L. D., S. L. Goldstein, S. R. Hemming, K. M. Jones, E. Calvo, C. Pelejero, and I. Cacho (2013), Rapid changes in meridional advection of Southern Ocean intermediate waters to the tropical Pacific during the last 30 kyr, *Earth Planet. Sci. Lett.*, *368*, 20–32.
Piotrowski, A. M., S. L. Goldstein, S. R. Hemming, and R. G. Fairbanks (2005), Temporal relationships of carbon cycling and ocean circulation at glacial boundaries, *Science*, *307*, 1933–1938, doi:10.1126/science.1104883.
Piotrowski, A. M., S. L. Goldstein, S. R. Hemming, R. G. Fairbanks, and D. R. Zylberberg (2008), Oscillating glacial northern and southern deep water formation from combined neodymium and carbon isotopes, *Earth Planet. Sci. Lett.*, *272*(1–2), 394–405, doi:10.1016/j.epsl.2008.05.011.
Piotrowski, A. M., A. Galy, J. A. L. Nicholl, N. Roberts, D. J. Wilson, J. A. Clegg, and J. Yu (2012), Reconstructing deglacial North and South Atlantic deep water sourcing using foraminiferal Nd isotopes, *Earth Planet. Sci. Lett.*, *357–358*, 289–297, doi:10.1016/j.epsl.2012.09.036.
Prospero, J. M., P. Ginoux, O. Torres, S. E. Nicholson, and T. E. Gill (2002), Environmental characterization of global sources of atmospheric soil dust identified with the nimbus 7 total ozone mapping spectrometer (TOMS) absorbing aerosol product, *Rev. Geophys.*, *40*(1), 1002, doi:10.1029/2000RG000095.
Rea, D. K. (1994), The paleoclimatic record provided by eolian deposition in the deep sea: The geologic history of wind, *Rev. Geophys.*, *32*, 159–195.
Rea, D. K., et al. (2006), Broad region of no sediment in the southwest Pacific Basin, *Geology*, *34*(10), 873–876.
Reid, J. L., and R. J. Lynn (1971), On the influence of the Norwegian-Greenland and Weddell seas upon the bottom waters of the Indian and Pacific oceans, *Deep Sea Res. Oceanogr. Abstr.*, *18*, 1063–1088.
Reimer, P. J., et al. (2013), IntCal13 and MARINE13 radiocarbon age calibration curves 0–50000 years calBP, *Radiocarbon*, *55*(4), 1869–1887, doi:10.2458/azu_js_rc.55.16947.
Rempfer, J., T. F. Stocker, F. Joos, J. C. Dutay, and M. Siddall (2011), Modelling Nd isotopes with a coarse resolution ocean circulation model: Sensitivities to model parameters and source/sink distributions, *Geochim. Cosmochim. Acta*, *75*, 5927–5950.
Rempfer, J., T. F. Stocker, F. Joos, and J.-C. Dutasy (2012), Sensitivity of Nd isotopic composition in seawater to changes in Nd sources and paleoceanographic implications, *J. Geophys. Res.*, *117*, C12010, doi:10.1029/2012JC008161.
Revel-Rolland, M., P. De Deckker, B. Delmonte, P. P. Hesse, J. W. Magee, I. Basile-Doelsch, F. Grousset, and D. Bosch (2006), Eastern Australia: A possible source of dust in East Antarctica interglacial Ice, *Earth Planet. Sci. Lett.*, *249*, 1–13.
Rickli, J., M. Frank, and A. N. Halliday (2009), The hafnium neodymium isotopic composition of Atlantic seawater, *Earth Planet. Sci. Lett.*, *280*, 118–127, doi:10.1016/j.epsl.2009.01.026.
Rickli, J., M. Gutjahr, D. Vance, M. Fischer-Gödde, C.-D. Hillenbrand, and G. Kuhn (2014), Neodymium and hafnium boundary contributions to seawater along the West Antarctic continental margin, *Earth Planet. Sci. Lett.*, *394*, 99–110.

Roberts, N. L., A. M. Piotrowski, J. F. McManus, and L. D. Keigwin (2010), Synchronous deglacial overturning and water mass source changes, *Science*, *327*, 75–78, doi:10.1126/science.1178068.
Roberts, N. L., A. M. Piotrowski, H. Elderfield, T. I. Eglinton, and M. W. Lomas (2012), Rare earth element association with foraminifera, *Geochim. Cosmochim. Acta*, *94*, 57–71.
Rosenthal, Y., M. P. Field, and R. M. Sherrell (1999), Precise determination of element/calcium ratios in calcareous samples using sector field inductively coupled plasma mass spectrometry, *Anal. Chem.*, *71*, 3248–3253, doi:10.1021/ac981410x.
Roy, M., T. van der Flierdt, S. R. Hemming, and S. L. Goldstein (2007), $^{40}Ar/^{39}Ar$ ages of hornblade grains and bulk Sm/Nd isotopes of circum-Antarctic glacio-marine sediments: Implications for sediment provenance in the southern ocean, *Chem. Geol.*, *244*, 507–519.
Rutberg, R. L., S. R. Hemming, and S. L. Goldstein (2000), Reduced North Atlantic deep water flux to the glacial Southern Ocean inferred from neodymium isotope ratios, *Nature*, *405*, 935–938, doi:10.1038/35016049.
Scher, H. D., and E. E. Martin (2004), Circulation in the Southern Ocean during the Paleogene inferred from neodymium isotopes, *Earth Planet. Sci. Lett.*, *228*, 391–405, doi:10.1016/j.epsl.2004.10.016.
Schmitz, W., A. Mangini, P. Stoffers, G. P. Glasby, and W. L. Pluger (1986), Sediment accumulation rates in the Southwestern Pacific Basin and Aitutaki Passage, *Mar. Geol.*, *73*, 181–190.
SCOR Working Group (2007), Geotraces—An international study of the global marine biogeochemical cycles of trace elements and their isotopes, *Chem. Erde Geochem.*, *67*(2), 85–131.
Siddall, M., S. Khatiwala, T. van de Flierdt, K. Jones, S. L. Goldstein, S. Hemming, and R. F. Anderson (2008), Towards explaining the Nd paradox using reversible scavenging in an ocean general circulation model, *Earth Planet. Sci. Lett.*, *274*, 448–461.
Singh, S. P., S. K. Singh, V. Goswami, R. Bhushan, and V. K. Rai (2012), Spatial distribution of dissolved neodymium and ε_{Nd} in the Bay of Bengal: Role of particulate matter and mixing of water masses, *Geochim. Cosmochim. Acta*, *94*, 38–56.
Soulet, G., G. Ménot, G. Bayon, F. Rostek, E. Ponzevera, S. Toucanne, G. Lericolais, and E. Bard (2013), Abrupt drainage cycles of the Fennoscandian Ice Sheet, *Proc. Natl. Acad. Sci. U. S. A.*, *110*, 6682–6687, doi:10.1073/pnas.1214676110.
Stancin, A. M., J. D. Gleason, S. A. Hovan, D. K. Rea, R. M. Owen, T. C. Moore Jr., C. M. Hall, and J. D. Blum (2008), Miocene to recent eolian dust record from the Southwest Pacific Ocean at 40°S latitude, *Palaeogeogr. Palaeoclimatol. Palaeoecol.*, *261*, 218–233.
Stern, C. R., and R. Kilian (1996), Role of the subducted slab, mantle wedge and continental crust in the generation of adakites from the Andean Austral volcanic zone, *Contrib. Mineral. Petrol.*, *123*, 163–281.
Stichel, T., M. Frank, J. Rickli, and B. A. Haley (2012a), The hafnium and neodymium isotope composition of seawater in the Atlantic sector of the Southern Ocean, *Earth Planet. Sci. Lett.*, *317*, 282–294.
Stichel, T., M. Frank, J. Rickli, E. C. Hathorne, B. A. Haley, C. Jeandel, and C. Pradoux (2012b), Sources and input mechanisms of hafnium and neodymium in surface waters of the Atlantic sector of the Southern Ocean, *Geochim. Cosmochim. Acta*, *94*, 22–37.
Stuiver, M., and H. A. Polach (1977), Reporting of C-14 Data—Discussion, *Radiocarbon*, *19*(3), 355–363.
Stuiver, M., and P. J. Reimer (1993), Extended C-14 data-base and revised Calib 3.0 C-14 age calibration program, *Radiocarbon*, *35*(1), 215–230.
Stumpf, R., M. Frank, J. Schönfeld, and B. A. Haley (2010), Late Quaternary variability of Mediterranean outflow water from radiogenic Nd and Pb isotopes, *Quat. Sci. Rev.*, *29*(19/20), 2462–2472, doi:10.1016/j.quascirev.2010.06.021.
Stumpf, R., M. Frank, J. Schönfeld, and B. A. Haley (2011), Climatically driven changes in sediment supply on the SW Iberian shelf since the Last Glacial Maximum, *Planet. Sci. Lett.*, *312*, 80–90.
Tachikawa, K., V. Athias, and C. Jeandel (2003), Neodymium budget in the modern ocean and paleo-oceanographic implications, *J. Geophys. Res.*, *108*(C8), 3254, doi:10.1029/1999JC000285.
Tachikawa, K., M. Roy-Barman, A. Michard, D. Thouron, D. Yeghicheyan, and C. Jeandel (2004), Neodymium isotopes in the Mediterranean Sea: Comparison between seawater and sediment signals, *Geochim. Cosmochim. Acta*, *68–14*, 3095–3106.
Tachikawa, K., A. M. Piotrowski, and G. Bayon (2014), Neodymium associated with foraminiferal carbonate as a recorder of seawater isotopic signatures, *Quat. Sci. Rev.*, *88*, 1–13, doi:10.1016/j.quascirev.2013.12.027.
Tanaka, T., et al. (2000), JNdi-1: A neodymium isotopic reference in consistency with LaJolla neodymium, *Chem. Geol.*, *168*(3–4), 279–281, doi:10.1016/S0009-2541(00)00198-4.
Tanaka, T. Y., and M. Chiba (2006), A numerical study of the contributions of dust source regions to the global dust budget, *Global Planet. Change*, *52*, 88–104.
Taylor, S. R., and S. M. McLennan (1985), *The Continental Crust: Its Composition and Evolution, An Examination of the Geochemical Record Preserved in Sedimentary Rocks*, 312 pp., Blackwell, Oxford, U. K.
Taylor, S. R., S. M. McLennan, and M. T. McCulloch (1983), Geochemistry of loess, continental crustal composition and crustal model ages, *Cosmochim. Acta*, *47*, 1897–1905.
Thiede, J. (1979), Wind regimes over the late Quaternary southwest Pacific Ocean, *Geology*, *7*, 259–262.
Tiedemann, R., F. Lamy, and Cruise Participants (2014), FS Sonne Fahrtbericht/Cruise report SO213—SOPATRA: South Pacific paleoceanographic transects—Geodynamic and climatic variability in space and time, Leg 1: Valparaiso/Chile - Valparaiso/Chile, 27.012.2010 - 12.01.2011, Leg 2: Valparaiso/Chile - Wellington/New Zealand, 12.01.2011 - 07.03.2011, Alfred Wegener Inst., Helmholtz Cent. for Polar and Mar. Res., Bremerhaven, Germany, doi:10.2312/cr_so213.
Tütken, T., A. Eisenhauer, B. Wiegand, and B. T. Hansen (2002), Glacial–interglacial cycles in Sr and Nd isotopic composition of Arctic marine sediments triggered by the Svalbard/Barents Sea ice sheet, *Mar. Geol.*, *182*, 351–372.
van de Flierdt, T., L. F. Robinson, and J. F. Adkins (2010), Deep-sea coral aragonite as a recorder for the neodymium isotopic composition of seawater, *Geochim. Cosmochim. Acta*, *74*, 6014–6032.
von Blanckenburg, F. (1999), Tracing past ocean circulation?, *Science*, *286*, 1862–1863.
Walter, H. J., E. Hegner, B. Diekmann, G. Kuhn, and M. M. R. Van Der Loeff (2000), Provenance and transport of terrigenous sediment in the South Atlantic Ocean and their relations to glacial and interglacial cycles: Nd and Sr isotopic evidence, *Geochim. Cosmochim. Acta*, *64*, 3813–3827.
Wandres, A. M., J. D. Bradshaw, S. Weaver, R. Maas, T. Ireland, and N. Eby (2004), Provenance analysis using conglomerate clast lithologies: A case study from the Pahau terrane of New Zealand, *Sediment. Geol.*, *167*, 57–89.
Warren, B. A. (1973), Transpacific hydrographic sections at latitudes 43°S and 28°S: The SCORPIO expedition—II. Deep water, *Deep Sea Res. Oceanogr. Abstr.*, *20*, 9–38.
Wilson, D. J., A. M. Piotrowski, A. Galy, and I. N. McCave (2012), A boundary exchange influence on deglacial neodymium isotope records from the deep western Indian Ocean, *Earth Planet. Sci. Lett.*, *341–344*, 35–47.
Wilson, D. J., A. M. Piotrowski, A. Galy, and J. A. Clegg (2013), Reactivity of neodymium carriers in deep sea sediments: Implications for boundary exchange an paleoceanography, *Geochim. Cosmochim. Acta*, *109*, 197–221.
Windom, H. L. (1970), Contribution of atmospherically transported trace metals to South Pacific sediments, *Geochim. Cosmochim. Acta*, *34*, 509–514.